Integrating Complex Covariate Transformations in Generalized Additive Models

Claudia Collarin,
Department of Environmental Sciences, Informatics and Statistics,
Ca' Foscari University of Venice,

Matteo Fasiolo, School of Mathematics, University of Bristol,

> Yannig Goude, Électricité de France R&D,

Simon N. Wood School of Mathematics, University of Edinburgh

Abstract

Transformations of covariates are widely used in applied statistics to improve interpretability and to satisfy assumptions required for valid inference. More broadly, feature engineering encompasses a wider set of practices aimed at enhancing predictive performance, and is typically performed as part of a data pre-processing step. In contrast, this paper integrates a substantial component of the feature engineering process directly into the modelling stage. This is achieved by introducing a novel general framework for embedding interpretable covariate transformations within multiparameter Generalised Additive Models (GAMs). Our framework accommodates any sufficiently differentiable scalar-valued transformation of potentially high-dimensional and complex covariates. These transformations are treated as integral model components, with their parameters estimated jointly with regression coefficients via maximum a posteriori (MAP) methods, and joint uncertainty quantified via approximate Bayesian techniques. Smoothing parameters are selected in an empirical Bayes framework using a Laplace approximation to the marginal likelihood, supported by efficient computation based on implicit differentiation methods. We demonstrate the flexibility and practical value of the proposed methodology through applications to forecasting electricity net-demand in Great Britain and to modelling house prices in London. The proposed methods are implemented by the gamFactory R package, available at https://github.com/mfasiolo/gamFactory.

Keywords: Generalized Additive Models; Covariate Transformations; Feature Engineering; Smoothing Splines; Functional Data; Distributional Regression.

1 Introduction

Transformations of independent variables are a standard tool in applied statistics. They involve modifying covariates to enhance the interpretability of statistical models or to satisfy assumptions that are essential for valid inference. While covariate transformations focus on altering existing variables, feature engineering encompasses a broader set of practices (Verdonck et al., 2024), including the creation of new variables and the application of dimension reduction techniques, and typically places greater emphasis on predictive performance. In most cases, both variable transformations and feature engineering are carried out as part of the pre-processing stage, that is, prior to fitting the chosen model.

In contrast, the present work aims to fully integrate part of the feature engineering process into the modelling phase. We focus particularly on interpretable transformations designed to handle complex covariates, such as time series and spatial data, and on their embedding into multi-parameter generalised additive models (GAMs), which include generalised additive models for location, scale and shape (GAMLSS; Rigby and Stasinopoulos, 2005) as a special case. In particular, we extend GAMs to accommodate smooth effects that incorporate any scalar-valued, nested covariate transformation that is sufficiently differentiable w.r.t. its own parameters. These transformations are treated as integral components of the model, with their parameters estimated jointly with the regression coefficients using maximum a posteriori (MAP) methods. Joint uncertainty estimates are obtained via approximate Bayesian methods. Smoothing parameters are selected within an empirical Bayes framework by maximising a Laplace approximation to the marginal likelihood (LAML) using quasi-Newton optimisation. As this procedure requires evaluation of the LAML gradient, we provide efficient methods for computing it by extending the implicit differentiation techniques of Wood et al. (2016) to exploit the specific structure of the models considered here. Additionally, we propose a principled and theoretically well-founded solution to the scaling problem that arises when constructing spline-based smooth effects of parameter-dependent covariate transformations.

The model class proposed here is widely applicable, but was initially motivated by problems in forecasting electricity net-demand, that is, consumption minus embedded generation. Consider the problem of forecasting the total hourly net-demand, y_t , in Great Britain (GB) using, among other covariates, a hourly forecast of external temperature, temp_t. Owing to buildings' thermal inertia, the consumption due to electrical heating and cooling at time t is not entirely driven by temp_t, but depends on temp_{t-1}, temp_{t-2}, ..., as well. One way to capture thermal inertia is to include in the forecasting model an exponentially smoothed temperature covariate, temp_t. An example is provided by the top row of Figure 1, which shows two smoothed temperature trajectories (left) and their effects on the expected net-demand (right). Here, estimating the exponential smoothing parameter during model fitting, rather than via expert knowledge, allowed us to identify a temperature effect characterised by low inertia (red), related to both heating and cooling, and a smoother one (blue), related to heating only. The effects correspond to a model described in Section 4.1.

As a further example, consider a London house prices modelling application, which will be described in detail in Section 4.2. Spatial residual autocorrelation is often strong in house prices due to unobservable local characteristics, events such as gentrification and foreclosures, as well as price spillover, that is, the effect of recently observed sale prices in

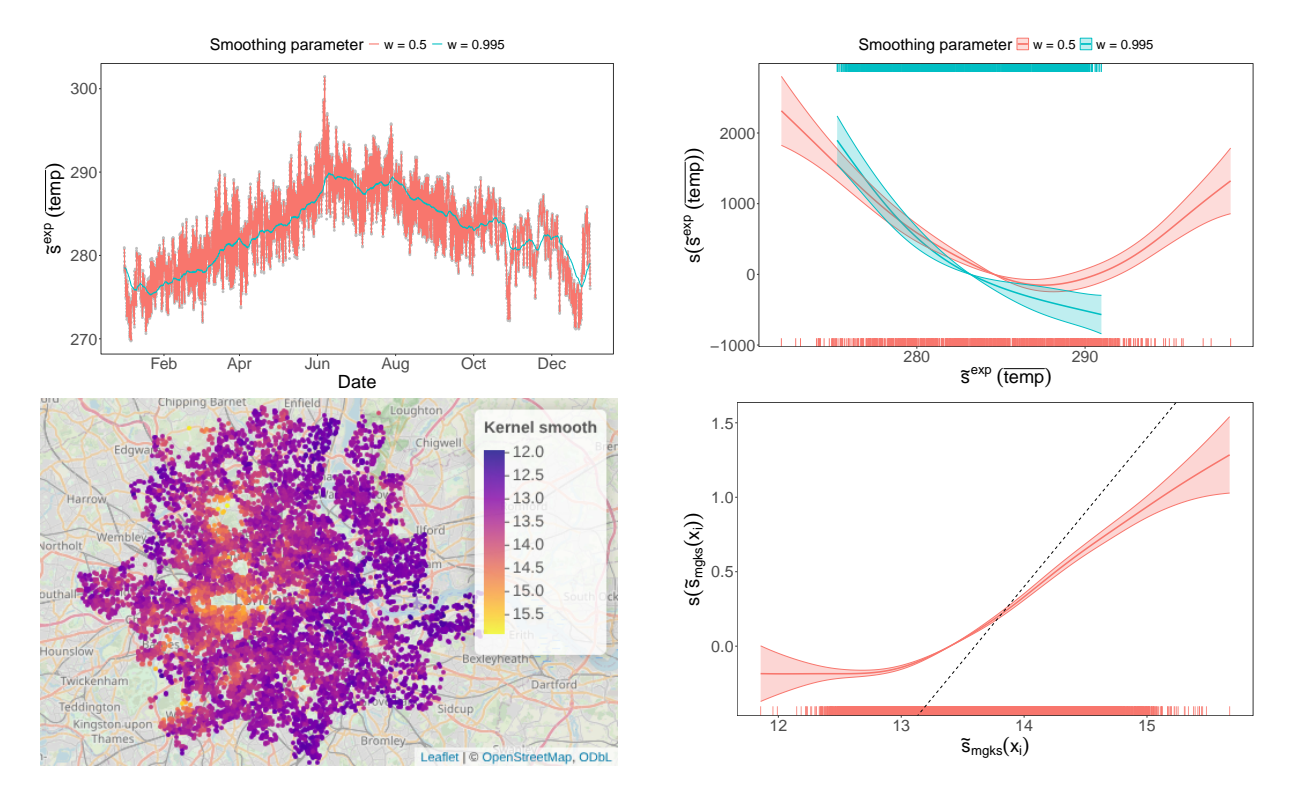


Figure 1: Examples of smooth effects with nested covariate transformations. Top row: Exponential smooths of forecast temperature in GB (left) and the corresponding smooth effects on electricity net-demand (right) for two distinct exponential smoothing parameters, estimated while fitting a model from Section 4.1. Bottom row: Estimated local house log-prices obtained by weighting neighbour prices via kernel smooth (left) and the corresponding effect on expected house log-prices (right), the dashed line has unit slope. The corresponding model is described in Section 4.2.

the neighbourhood (Kallberg and Shimizu, 2025; Guerrieri et al., 2013; Fischer et al., 2018). Spatial autoregressive models capture such effects by first weighting neighbouring sale prices to build a local price index, which is then considered fixed when fitting the regression model (LeSage and Pace, 2009). The methods proposed here allow to simultaneously select the rate of decay of the spatial weights and estimate the non-linear effect of the local weighted price index on expected prices. An example is provided by the bottom row of Figure 1, which shows the estimated local log-price index (left) and its effect on expected log-price (right), obtained on the London data.

To the best of our knowledge, the work proposed here is the first to fully integrate general covariate transformations within a GAM modelling framework. Nevertheless, covariate transformations have a long-standing history in statistics, and the automatic estimation of transformation parameters was first proposed by Box and Cox (1964). However, their work, and many subsequent developments such as Thompson (2003) and Fan et al. (2013), have focussed on finding transformations that linearise the relation between the response and the covariates. In contrast, here we flexibly capture non-linearities via smooth effects, and use nested covariate transformations to integrate the processing of complex covariates into the model.

From this perspective, functional GAMs (FGAMs, McLean et al., 2014; Greven and

Scheipl, 2017) provide an alternative to the methods proposed here in certain applications. Specifically, they provide GAM methods meant to incorporate functional covariates within the model, thus avoiding the use of a pre-processing step aimed at summarising them to scalar covariates. Similarly, penalised distributed lag effects (Zanobetti et al., 2000; Muggeo, 2008; Gasparrini et al., 2017) represent an alternative to smooth effects of linear combinations of covariates when capturing the effect of several lagged values of the same covariate. These effects are a special case of the class of transformations considered here and will be referred to as single index effects. Further, latent Gaussian models (Rue et al., 2009; Lindgren et al., 2011) can be used in place of the nested transformation provided here to capture spatio-temporal dependencies and correlations.

The model class proposed here is also closely related to projection pursuit regression (PPR, Friedman and Stuetzle, 1981; Collins et al., 2024) and (generalised) partially linear single index models (GPLISM, Carroll et al., 1997; Antoniadis et al., 2004; Liang et al., 2010; Yu et al., 2017). In particular, both model classes include single index effects. Hence, the proposed model class extends such models by offering a wider range of transformations, as well as by allowing for multiple linear predictors and response distributions beyond the exponential family.

The rest of the article is structured as follows. Section 2 introduces the proposed model structure, with three examples of covariate transformations, and gives details on how to address the scaling issue mentioned above. Section 3 focusses on the fitting, computational and inferential framework, while Section 4 considers applications to net-demand forecasting in GB and house prices modelling in London.

2 Integrating covariate transformations in GAMs

2.1 The general model structure

Let $\mathbf{y} = \{y_1, \dots, y_n\}$ be a vector of response variables and $\mathbf{x}_1, \dots \mathbf{x}_n$ the corresponding d-dimensional vectors of covariates. Assume that the y_i 's are conditionally independent and follow the distribution $\mathcal{D}(y_i; \boldsymbol{\theta}_i)$, with p.d.f. $p(y_i|\mathbf{x}_i)$. In what follows, a covariate transformation is a scalar-valued function $\tilde{s} : \mathbb{R}^p \to \mathbb{R}$ parameterised by a vector \boldsymbol{a} and fourth-order differentiable w.r.t. the latter. A nested smooth effect, s, is a fourth-order differentiable smooth function whose argument is a covariate transformation, that is, $s(\tilde{s}(\cdot))$. The elements of the parameter vector $\boldsymbol{\theta}_i$ are modelled by

$$g_{j}(\theta_{ji}) = \eta_{ji} = \left(\mathbf{Z}_{ji}^{0}\right)^{\mathsf{T}} \boldsymbol{\gamma}_{j0} + \sum_{k=1}^{K_{j}} f_{jk} \left(\mathbf{x}_{i}^{S_{jk}}\right) + \sum_{u=1}^{U_{j}} s_{ju} \left(\tilde{s}_{ju} \left(\mathbf{x}_{i}^{\tilde{S}_{ju}}\right)\right), \quad \text{for} \quad j = 1, \dots, m.$$

$$(1)$$

where g_j is a monotonic function, \mathbf{Z}_{ji}^0 is the *i*-th row of the design matrix \mathbf{Z}_j^0 , and γ_{j0} is a vector of regression coefficients. We indicate standard smooth terms with $f_{jk}(\cdot)$ and nested smooth effects with $s_{ju}(\tilde{s}_{ju}(\cdot))$. The covariates that each smooth depends on are denoted by $\mathbf{x}_i^{S_{ju}}$, where, $S_{ju} \subseteq \{1,\ldots,d\}$. For example, if $S_{ju} = \{1,3\}$, then $\mathbf{x}_i^{S_{ju}}$ is a two-dimensional vector consisting of the first and third elements of \mathbf{x}_i . Each function f_{jk}

is built via

$$f_{jk}\left(\mathbf{x}_{i}^{S_{jk}}\right) = \sum_{l=1}^{L_{jk}} h_{l}^{jk}\left(\mathbf{x}_{i}^{S_{jk}}\right) \gamma_{l}^{jk} \tag{2}$$

where h_l^{jk} are basis function of dimension $|S_{jk}|$ and γ_l^{jk} are regression coefficients. Each s_{ju} is built via a linear combination of spline basis functions, as in (2), with the additional requirement that the basis functions must be fourth-order differentiable. This is imposed by the efficient fitting framework described in Section 3. While the argument of s_{ju} depends on a^{ju} , the basis functions themselves (e.g., the position of the knots) should not depend on a^{ju} . See Section 2.3 for more details. Any basis function that meets the above requirements can be used to construct s_{ju} , and there are no restrictions for f_{jk} .

The number of basis functions used to build each f_{jk} and s_{ju} is chosen to be large enough to avoid over-smoothing. The wiggliness of these effects is controlled by an improper multivariate Gaussian prior on the regression coefficients. The prior is centred at zero and shrinks the effects toward smoothness, where the definition of smoothness depends on the specific effect and prior applied. The prior precision matrix is $\mathbf{S}^{\lambda} = \sum_{g=1}^{G} \lambda_g \mathbf{S}_g$, with each \mathbf{S}_g being a positive semidefinite matrix and $\lambda = \{\lambda_1, ..., \lambda_G\}$ a vector of positive smoothing parameters. The prior can also include the parameters of the \tilde{s}_{ju} 's. However, its interpretation depends on the type of transformation and prior considered.

2.2 Instances of covariate transformations

Here we detail three instances of nested transformation, namely adaptive exponential smoothing, multivariate kernel smoothing and linear combinations.

2.2.1 Adaptive exponential smoothing

Let x_i be the *i*-th observed value of a scalar covariate. An adaptive exponential smoothing transformation is

$$\tilde{s}(x_i) = \tilde{s}_i = \omega_i \tilde{s}_{i-1} + (1 - \omega_i) x_i, \quad \text{for} \quad i \ge 1,$$

where $\tilde{s}_0 = x_0$ and $\omega_i \in (0, 1)$. The smoothing factor can be modelled via $\omega_i = \phi(\tilde{\mathbf{x}}_i^{\mathsf{T}} \boldsymbol{a})$, where ϕ is the logistic function, $\tilde{\mathbf{x}}_i$ is a fixed vector, and \boldsymbol{a} is a vector of parameters. In Section 4.1 we provide an example where ω depends on $\tilde{\mathbf{x}}_i^{\mathsf{T}} = [1, \Delta h_i - 1]$, where Δh_i is the time interval in hours between the observation i and i-1. In principle ω could be either constant or modelled via a full additive model, involving the sum of several parametric and penalised, non-parametric effects. The logistic function is used to ensure that $\omega_i \in (0,1)$, but in principle any unconstrained, fourth-order differentiable parametrisation could be used. The top-left plot in Figure 1 shows an example of an exponential smoothing transformation.

2.2.2 Multivariate kernel smoothing

Let z_i be a scalar covariate corresponding to the vector \mathbf{x}_i . For example, z_i might be the temperature measured at the location \mathbf{x}_i . A kernel smooth of z, evaluated at \mathbf{x}_i , is

$$\tilde{s}(\mathbf{x}_i) = \frac{\sum_{j \in \mathcal{N}_i} K_{\mathbf{a}}(\mathbf{x}_i, \mathbf{x}_j) z_j}{\sum_{q \in \mathcal{N}_i} K_{\mathbf{a}}(\mathbf{x}_i, \mathbf{x}_q)},\tag{4}$$

where K_a is the kernel of a multivariate p.d.f., parametrised by vector \mathbf{a} and \mathcal{N}_i is the set of indices of \mathbf{x}_i 's neighbours. Note that i might not appear in \mathcal{N}_i , an example being provided by the application discussed in Section 4.2, where kernel smoothing estimates of house prices are obtained from neighbouring prices. More generally, this transformation can be useful when dealing with misaligned covariates, which are recorded at locations different from those of the response variable.

In this work we consider the multivariate Gaussian kernel with bandwidth matrix Σ where $a_k = \log(1/\Sigma_{kk})$ and $\Sigma_{jk} = 0$ for $j \neq k$. We do not consider adaptive smoothing, but in principle this could be done by modelling the diagonal elements of Σ via an additive model, as we did for exponential smoothing. Further, one might consider modelling the full bandwidth matrix by, for example, using a to control its Cholesky factor. The fitting methods in Section 3 would support such a model, but we leave this to future work.

2.2.3 Linear combinations

Let \mathbf{x}_i be a vector of covariates; the linear combination

$$\tilde{s}(\mathbf{x}_i) = \mathbf{x}_i^\mathsf{T} \boldsymbol{a} \tag{5}$$

allows for the inclusion of single index effects, i.e. smooth functions of linear combinations, into the model. Such transformations can be used to perform dimension reduction. Specifically, under the fitting framework proposed here, it is possible to specify interpretable multivariate Gaussian priors on the coefficient vector \mathbf{a} , which can be advantageous when \mathbf{a} is high-dimensional. For example, in Section 4.1 the elements of \mathbf{a} are used to form a distributed lag effect, hence we use a prior penalising $\sum_{k}(a_k - a_{k-1})^2$, meant to encourage smoothness between the coefficients of consecutive lags. While we do not provide examples here, note that the elements of \mathbf{x}_i could be the evaluated spline basis functions of some covariate z_i , i.e. $\mathbf{x}_i = \mathbf{x}(z_i)$, or more generally the *i*-th row of the model matrix of an additive model. That is, linear combinations can be used to build smooth effects whose argument is itself an additive model.

From a computational perspective, linear combinations are a special case of transformations, because the linearity between \tilde{s} and a makes the derivative system simple and more efficient to compute with, as explained in Section 3. However, there are simple non-linear variants of (5) that are compatible with the fitting framework provided here and could be considered in future work. For instance, \tilde{s} could be a shape-constrained smooth effect, constructed using one of the non-linear parametrisations proposed by Pya and Wood (2015). Alternatively, if x_{ij} is a covariate measured at time t_{i-j} , with $j=1,2,\ldots$, one might want to impose $|a_1|>|a_2|>\ldots$, so that the weights of past covariates must decrease with the time lag. Such a constrained distributed lag effect could be implemented by adopting the parametrisation $a_1=\tilde{a}_1$ and $a_j=a_{j-1}\phi(\tilde{a}_j)$, where each \tilde{a}_j is unconstrained and $\phi:\mathbb{R}\to (-1,1)$ is a monotonic and differentiable function.

2.3 Nested smooth effect specification and identifiability

Integrating smooth effects with nested transformations within the empirical Bayes fitting framework adopted here presents additional challenges, relative to standard smooth effects. While in Section 3 we address the non-linearity of a nested effect, $s(\tilde{s}(\mathbf{x}))$, w.r.t. the transformation's parameters, \boldsymbol{a} , here we focus on scaling and knots-placement issues.

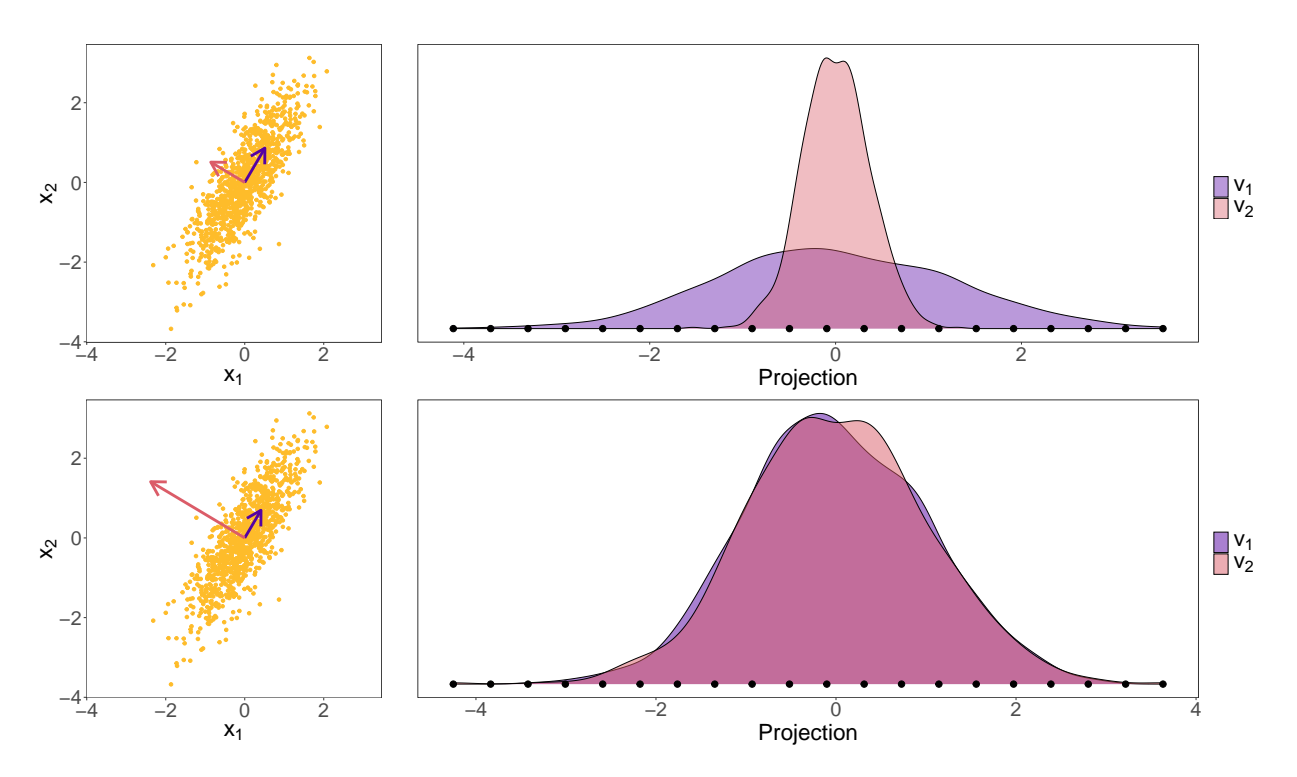


Figure 2: Scaling issues in linear combinations. Top row: Scatterplot plot of data to be combined via two unit-vectors (left) and densities of the transformed data (right). Bottom rows: Same as on the top row, but here the norm of the vectors is adjusted to renders the scale of the transformed data invariant w.r.t. the direction of the combination vector.

2.3.1 The scaling problem

Assume, for simplicity, that the outer smooth $s(\cdot)$ is built via a knot-based spline basis and note that the argument of $s(\cdot)$, i.e. $\tilde{s}(\mathbf{x})$, depends on \boldsymbol{a} . Hence, as \boldsymbol{a} is varied during model fitting, the spline basis functions are evaluated at different locations. For bases with finite support, such as B-splines, this creates an issue as there is no guarantee that all the values taken by $\tilde{s}(\mathbf{x})$ fall within the support of $s(\cdot)$, as \boldsymbol{a} varies. Also, the range of values taken by $\tilde{s}(\mathbf{x})$, might be much smaller than the knot range of $s(\cdot)$, so that only a few basis functions contribute to the fit, leading to computational inefficiency and undersmoothing. This scaling problem is not limited to knot-based bases and can not be solved by adopting knot-free spline bases, such as thin plate splines. In fact, regardless of the type of basis being used, the scale and range of the covariate of interest must be taken into account when constructing the basis for the corresponding smooth effect, but here the scale and range are a-dependent, not fixed as for standard, non-nested smooth effects. A naïve solution to this scaling problem would be to rebuild the spline basis as a changes, for example by using knots that are equally-spaced across the range of values taken by $\tilde{s}(\mathbf{x})$. However, doing so would violate the fourth-order differentiability requirements imposed by the fitting framework adopted here.

To get an intuition on the proposed solution, consider Figure 2, top row. The scatterplot represents sample vectors \mathbf{x}_i , to be linearly combined via $\tilde{s}(\mathbf{x}) = \mathbf{x}^\mathsf{T} \boldsymbol{a}$, with $||\mathbf{a}|| = 1$. The densities on the right represent the distribution of the projected data and show that it depends on the direction of \boldsymbol{a} . Hence, a spline basis for the outer smooth $s(\cdot)$ with support

on, say, [-2, 2] would be too (wide) narrow when \boldsymbol{a} is parallel to the (minor) major axis of the data ellipse. However, the second row of Figure 2 shows that the scale of $\tilde{s}(\mathbf{x})$ can be made invariant by rescaling the norm of \boldsymbol{a} based on its direction.

This idea can be extended to a general transformation, $\tilde{s}(\mathbf{x})$, by imposing the constraints mean $[\tilde{s}(\mathbf{x})] = 0$ and var $[\tilde{s}(\mathbf{x})] = 1$ on its sample mean and variance. While practical details on how to implement such constraints are provided in Appendix S1, below we explain how standardising the transformation helps to choose the range of knot-based outer smooth effects.

2.3.2 Choosing the extreme knots

Indicate $\tilde{s}(\mathbf{x}_i)$, where \mathbf{x}_i is the *i*-th observed covariate value, simply with \tilde{s}_i , for i = 1, ..., n. Similarly, use $\tilde{S}_{n+1} = \tilde{s}(\mathbf{X}_{n+1})$ to indicate the transformation of a new, unobserved random covariate (e.g., from a test set). Assume that the sample mean and variance of \tilde{s}_i are fixed respectively to 0 and to some arbitrary positive constant c.

Focusing on symmetric knot ranges of the type $\mathcal{R}(\xi) = [-\xi\sqrt{c}, \xi\sqrt{c}]$, we chose the value of $\xi > 0$ based on a deterministic upper bound, π , on the proportion of s_i 's that falls outside of $\mathcal{R}(\xi)$. In particular, assuming for simplicity that $\pi n/2$ is an integer, then the choice $\xi = \sqrt{(2-\pi)/\pi}$ guarantees that at most πn of the observations will fall outside of $\mathcal{R}(\xi)$. Further, the probability that a new transformed covariate, \tilde{S}_{n+1} , falls outside of $\mathcal{R}(\xi)$ can be upper bounded by

$$\mathbb{P}\left(\tilde{S}_{n+1} \notin \mathcal{R}(\xi)\right) < \frac{1}{n+2} \left| \frac{n+2}{n+1} \left(\frac{n}{\xi^2} + 1 \right) \right| = \frac{\pi}{2-\pi} + O(n^{-1}), \quad \text{with} \quad \xi = \sqrt{\frac{2-\pi}{\pi}}.$$

The probabilistic bound involving \tilde{S}_{n+1} is a direct application of the finite sample version of Chebyshev's inequality (Kabán, 2012). The deterministic bound is obtained by applying the extension of Samuelson's inequality obtained by Wolkowicz and Styan (1979) which, given the constraints on the sample mean and variance, guarantees that the k-th order statistic of $(\tilde{s}_1, \ldots, \tilde{s}_n)$ falls in $[-\sqrt{c(n-k)/k}, \sqrt{c(k-1)/(n-k+1)}]$, for any $k=1,\ldots,n$. Setting $k=\pi n/2$, implies that at most πn observations will fall outside the interval $[-\sqrt{c(2-\pi)/\pi}, \sqrt{c(2-\pi)/\pi}]$. If $\pi n/2$ is non-integer, then setting $k=\lfloor \pi n/2 \rfloor$ leads to at most $\lfloor \pi n \rfloor$ observations outside $\mathcal{R}(\xi)$.

Note that bounds provided above do not make any assumption on the distribution of the \mathbf{x}_i 's, hence they are fairly pessimistic. For example, in the applications discussed in Sections 4.1 and 4.2 we place the extreme knots using $\xi = 6$ and c = 1, which leads to $\pi \approx 0.05$ and $\pi/(2-\pi) \approx 0.025$. However, no transformed covariate in the in-sample and out-of-sample data falls outside $\mathcal{R}(\xi)$, under both models.

2.3.3 Constraints on the outer effect

All the considerations discussed so far relate to the inner transformation \tilde{s} . Regarding the outer smooth effect, to ensure the identifiability of it, we imposed a set of point and derivative constraints. Specifically, the smooth was constrained to have no intercept, that is, s(0) = 0. This restriction avoids directly orthogonalising the smooth to the intercept term, i.e. $\sum_{i} s(\tilde{s}(x_i)) = 0$, which would require the knowledge of $\tilde{s}(\mathbf{x})$ before starting the

fitting procedure. In addition, outside the support $\mathcal{R}(\xi)$, we imposed a linear extrapolation of the smooth effect. The definition of $\mathcal{R}(\xi)$ implies that during the optimisation procedure, a subset of \tilde{s}_i 's may still fall beyond the support. Therefore, to satisfy the continuity assumptions, we imposed higher-order derivative constraints on the boundary knots, requiring $s^{(2)}(\kappa) = s^{(3)}(\kappa) = s^{(4)}(\kappa) = 0$ for $\kappa \in \{-\xi\sqrt{c}, \xi\sqrt{c}\}$.

3 Model fitting and inference

3.1 Fitting framework overview

Denote the vector containing all the regression coefficients and transformation parameters in the model with ζ and the log-likelihood corresponding to the *i*-th observation with $\ell_i(\zeta)$. Under the Gaussian prior described in Section 2.1 and the constraints on the sample variance of the nested transformations described in Section 2.3, the Bayesian posterior log-density can be expressed as

$$\mathcal{L}(\zeta) = \log p(\zeta | \boldsymbol{y}, \boldsymbol{\lambda}) = \sum_{i=1}^{n} \ell_i(\zeta | y_i) - \frac{1}{2} \sum_{g=1}^{G} \lambda_g \zeta^{\mathsf{T}} \mathbf{S}_g \zeta,$$
 (6)

up an additive constant. Under a multivariate Gaussian prior, the prior log-density is equivalent to a generalized ridge penalty. Consequently, high values of a smoothing parameter λ_g lead to a posterior distribution that is more concentrated on the null space of the penalty. The definition of this null space depends on the choice of the prior precision matrix \mathbf{S}_g . Once \mathbf{S}_g is chosen, it defines the concept of smoothness for the corresponding effect and the null space of "completely smooth" functions. Note that, in general, there is no one-to-one correspondence between the effects and the smoothing parameters. For instance, the wiggliness of an effect can be controlled using multiple smoothing parameters, while a single penalty can affect several effects.

For fixed smoothing parameters, λ , we obtain MAP estimates of the regression coefficients by maximising the log-posterior (6) via Newton's algorithm. However, the main challenge is selecting the smoothing parameters themselves. We do this by maximising an approximation to the log marginal likelihood, $V(\lambda) = \log p(\lambda) = \log \int p(y|\zeta)p(\zeta|\lambda)d\zeta$. In particular, we consider a Laplace approximate marginal likelihood (LAML) criterion

$$\tilde{\mathcal{V}}(\lambda) = \mathcal{L}(\hat{\zeta}) + \frac{1}{2}\log|\mathbf{S}^{\lambda}|_{+} - \frac{1}{2}\log|\mathcal{H}| + \frac{M_{p}}{2}\log(2\pi), \tag{7}$$

where M_p is the dimension of the null space of \mathbf{S}^{λ} , $|\mathbf{S}^{\lambda}|_{+}$ is the product of its positive eigenvalues, \mathcal{H} is the negative Hessian of (6), evaluated at its maximiser, $\hat{\boldsymbol{\zeta}}$. To ensure the positivity of $\boldsymbol{\lambda}$, we maximise (7) w.r.t. $\boldsymbol{\rho}$, where $\rho_g = \log(\lambda_g)$. We use a BFGS optimiser, which requires the gradient of the objective

$$(\nabla_{\boldsymbol{\rho}}\tilde{\mathcal{V}})_g = \frac{\partial \tilde{\mathcal{V}}}{\partial \rho_q} = -\frac{\lambda_g}{2}\hat{\boldsymbol{\zeta}}^\mathsf{T}\mathbf{S}_g\hat{\boldsymbol{\zeta}} + \frac{1}{2}\frac{\partial \log|\mathbf{S}^{\boldsymbol{\lambda}}|_+}{\partial \rho_q} - \frac{1}{2}\frac{\partial \log|\boldsymbol{\mathcal{H}}|}{\partial \rho_q}.$$
 (8)

Although computing the first two terms is straightforward, the third term is more involved. In particular, following Wood et al. (2016), we have

$$\frac{\partial \log |\mathcal{H}|}{\partial \rho_g} = \operatorname{tr}\left(\mathcal{H}^{-1} \frac{\partial \mathcal{H}}{\partial \rho_g}\right). \tag{9}$$

The direct calculation of (9) results in a computational cost of $O(np^3)$, where $p = \dim(\zeta)$, for each ρ_g . However, Wood et al. (2016) shows how to achieve a more efficient $O(np^2)$ for standard GAMLSS models. Attaining similar computational efficiency for models with nested transformations is more challenging, but in Section 3.2 we provide methods that are as efficient as possible.

3.2 Efficient and modular derivative computation

For simplicity of notation, consider a GAM characterised by a single parameter θ and a linear predictor $\eta = g(\theta)$. The general scenario leverages the block structure of the derivative system using the chain rule. The linear predictor is modelled via a parametric part, in addition to the K standard and the U nested smooth effects. Define the vector $\boldsymbol{\gamma} = [\boldsymbol{\gamma}_0^\mathsf{T}, \dots, \boldsymbol{\gamma}_K^\mathsf{T}]^\mathsf{T}$ of all the coefficients belonging to parametric and standard smooth effects, and let $\mathbf{Z} = [\mathbf{Z}^0, \mathbf{Z}^1, \dots, \mathbf{Z}^K]$ be the corresponding model matrix. As already mentioned in Section 2.2.3, linear combinations are an important special case from a computational perspective. Consequently, we divide the U effects into those based on linear combinations and the rest. Without loss of generality, assume that the first P nested smooths are based on linear combinations with weights $\boldsymbol{\alpha}_1, \dots, \boldsymbol{\alpha}_P$ and parameters of the outer spline bases $\boldsymbol{\beta}_1, \dots, \boldsymbol{\beta}_P$. Denote by $\boldsymbol{b}_1, \dots, \boldsymbol{b}_{U-P}$ and $\boldsymbol{a}_1, \dots, \boldsymbol{a}_{U-P}$ the outer and inner coefficients of the remaining nested effects, respectively.

To maximise (6) using Newton's method, we need first and second order derivatives w.r.t. all regression coefficients. Getting a compact, modular expression for the Hessian is the main challenge, and hence we adjust our notation accordingly. The Hessian is composed of (U+1)(U+2)/2 unique blocks, and the structure of the latter depends on the coefficients involved. In particular, we drop the indices and simply indicate with **a** and **b** the transformation and spline basis coefficients of one of the U-P nested effects. Let a_* and b_* indicate the coefficients of a different nested effect. For effects based on linear combinations, define α , α^* , β and β^* similarly. Consider the set of parameter vectors $C = \{\gamma, a, a_*, b, b_*, \alpha, \alpha_*, \beta, \beta_*\}$. In total, there are |C|(|C|+1)/2 = 45 unique pairs in C, which is the number of unique Hessian block types.

Here we provide the formulas for the gradient of the log-likelihood w.r.t. a generic vector $\psi \in \{\gamma, a, b, \alpha, \beta\}$ and for a Hessian block involving any pair $\{\psi_1, \psi_2\}$ in $C \times C$. To do this, we need a few more definitions. Let \mathbf{M}_b and \mathbf{M}_β be the model matrices corresponding to the outer splines basis of, respectively, a general nested effect and a nested effect based on a linear combination. These are the bases used to build an effect $s(\cdot)$ in (1). Let \mathbf{M}_a and \mathbf{M}_α be the matrices such that $\mathbf{M}_a = \nabla_a \tilde{\mathbf{s}}$ and $\mathbf{M}_\alpha = \nabla_\alpha \tilde{\mathbf{s}}$, where $\nabla_a \tilde{\mathbf{s}} = \partial \tilde{\mathbf{s}}/\partial a^{\mathsf{T}}$ and $\tilde{\mathbf{s}} = \tilde{s}(\mathbf{X}^{\tilde{s}})$ be the vector containing the n observed values of a transformation \tilde{s} . Note that $\mathbf{M}_\alpha = \mathbf{X}^{\tilde{s}}$, because the transformation is linear, see formula (5). Indicate with \mathbf{M}_b^t and \mathbf{M}_β^t the matrices such that $(M_b^t)_{ik} = \partial^t (M_b)_{ik}/\partial \tilde{s}_i^t$ and $(M_\beta^t)_{ik} = \partial^t (M_\beta)_{ik}/\partial \tilde{s}_i^t$, with $t = 1, 2, \ldots, n$. These are the derivatives of the outer splines bases of the nested effects w.r.t. the observed values of the transformation.

Let $\ell = \sum_i \ell_i$ be the log-likelihood and define the vector $\boldsymbol{\ell}$ such that its *i*-th element is ℓ_i . Indicate with $\boldsymbol{\ell}^{\xi_1}$, $\boldsymbol{\ell}^{\xi_1 \xi_2}$ and $\boldsymbol{\ell}^{\xi_1 \xi_2 \xi_3}$ the vectors such that $\ell_i^{\xi_1} = \partial \ell_i / \partial \xi_1$, $\ell_i^{\xi_1 \xi_2} = \partial^2 \ell_i / \partial \xi_1 \partial \xi_2$ and $\ell_i^{\xi_1 \xi_2 \xi_3} = \partial^3 \ell_i / \partial \xi_1 \partial \xi_2 \partial \xi_3$, with $\xi_i \in \{\eta, \theta, \tilde{s}\}$. Note that the formulas for $\xi = \theta$ are model-specific. That is, they depend on the distribution $\mathcal{D}(y_i; \boldsymbol{\theta}_i)$. Formulas for computing the (mixed) derivatives of ℓ w.r.t. η and \tilde{s} from the derivatives of ℓ and of the link function g w.r.t. θ are provided in Appendix S3. Define

$$p(\boldsymbol{\psi}) = \begin{cases} \eta & \boldsymbol{\psi} \in \{\boldsymbol{\gamma}, \boldsymbol{\beta}, \boldsymbol{b}\} \\ \tilde{s}_{\boldsymbol{\psi}} & \boldsymbol{\psi} \in \{\boldsymbol{\alpha}, \boldsymbol{a}\}, \end{cases}$$

then, $\ell^{p(\psi)}$ indicate ℓ^{η} if $\psi \in \{\gamma, \beta_p, \boldsymbol{b}_u\}$ or $\ell^{\tilde{s}_{\psi}}$ if $\psi \in \{\boldsymbol{\alpha}_p, \boldsymbol{a}_u\}$. To make the notation more compact, we write $p(\psi_1, \psi_2)$ and $p(\psi_1, \psi_2, \psi_3)$ instead of $p(\psi_1)p(\psi_2)$ and $p(\psi_1)p(\psi_2)p(\psi_3)$.

3.2.1 Gradient and Hessian of the log-likelihood

Under the notation just described, all the vectors forming the gradient for the log-likelihood follow the general pattern $\nabla_{\psi} \ell = \mathbf{M}_{\psi}^{\mathsf{T}} \ell^{p(\psi)}$. In the Hessian matrix, most of the block types follow the pattern

$$\frac{\partial^2 \ell}{\partial \boldsymbol{\psi}_1^\mathsf{T} \partial \boldsymbol{\psi}_2} = \mathbf{M}_{\boldsymbol{\psi}_2}^\mathsf{T} \mathbf{H}^{\boldsymbol{\psi}_1 \boldsymbol{\psi}_2} \mathbf{M}_{\boldsymbol{\psi}_1},$$

where $\mathbf{H}^{\psi_1\psi_2}$ is a diagonal matrix with non-zero elements $(\mathbf{H}^{\psi_1\psi_2})_{ii} = \ell_i^{p(\psi_1,\psi_2)}$. Block types that do not follow the general pattern are

$$\begin{split} & \nabla_{\boldsymbol{\alpha}}^{\mathsf{T}} \nabla_{\boldsymbol{\beta}} \ell = \mathbf{M}_{\boldsymbol{\beta}}^{\mathsf{T}} \operatorname{diag}\left(\boldsymbol{\ell}^{\eta \tilde{s}}\right) \mathbf{M}_{\boldsymbol{\alpha}} + (\mathbf{M}_{\boldsymbol{\beta}}^{1})^{\mathsf{T}} \operatorname{diag}\left(\boldsymbol{\ell}^{\eta}\right) \mathbf{M}_{\boldsymbol{\alpha}}, \\ & \nabla_{\boldsymbol{a}}^{\mathsf{T}} \nabla_{\boldsymbol{a}} \ell = \mathbf{M}_{\boldsymbol{a}}^{\mathsf{T}} \operatorname{diag}\left(\boldsymbol{\ell}^{\tilde{s}\tilde{s}}\right) \mathbf{M}_{\boldsymbol{a}} + \sum_{i=1}^{n} \ell_{i}^{\tilde{s}} \nabla_{\boldsymbol{a}}^{\mathsf{T}} \nabla_{\boldsymbol{a}} \tilde{s}_{i}, \\ & \nabla_{\boldsymbol{a}}^{\mathsf{T}} \nabla_{\boldsymbol{b}} \ell = (\mathbf{M}_{\boldsymbol{b}})^{\mathsf{T}} \operatorname{diag}\left(\boldsymbol{\ell}^{\eta \tilde{s}}\right) \mathbf{M}_{\boldsymbol{a}} + (\mathbf{M}_{\boldsymbol{b}}^{1})^{\mathsf{T}} \operatorname{diag}\left(\boldsymbol{\ell}^{\eta}\right) \mathbf{M}_{\boldsymbol{a}}. \end{split}$$

Note that all non-standard blocks are derivatives of a nested effect w.r.t. its parameters, and that $\nabla_{\alpha}^{\mathsf{T}} \nabla_{\alpha} \ell$ follows the standard pattern since $\nabla_{\alpha}^{\mathsf{T}} \nabla_{\alpha} \tilde{s}_i = 0$ for any $i = 1, \ldots, n$.

3.2.2 Derivatives of Hessian blocks

Here we explain how to compute the derivative of the Hessian blocks w.r.t. a log smoothing parameters $\rho = \log \lambda$. Let m be the total number of γ , α , β , a and b vectors contained in the model. Let us indicate with

$$\frac{\partial \nabla_{\boldsymbol{\psi}_{j}}^{\mathsf{T}} \nabla_{\boldsymbol{\psi}_{k}} \ell}{\partial \rho} = \sum_{l=1}^{K_{l}} \frac{\partial \nabla_{\boldsymbol{\psi}_{j}}^{\mathsf{T}} \nabla_{\boldsymbol{\psi}_{k}} \ell}{\partial \hat{\boldsymbol{\psi}}_{l}} \frac{\partial \hat{\boldsymbol{\psi}}_{l}}{\partial \rho} = \sum_{l=1}^{K_{l}} \boldsymbol{\Gamma}_{l}^{jk},$$

the derivative of a Hessian block w.r.t. a log-smoothing parameter, where K_l is the number of elements of ψ_l . The terms Γ_l^{jk} indicate the partial effect of the log-smoothing parameter ρ on the j-k block of Hessian via the l-th vector of coefficients.

As before, let us assume for simplicity that the model contains a single linear predictor η , modelled via two general nested effects, two single index effects, and one standard smooth effect. Then we indicate Γ_l^{jk} simply with Γ_3^{12} . Most such terms follow the general pattern

$$\mathbf{\Gamma}_3^{12} = \mathbf{M}_{\boldsymbol{\psi}_2}^\mathsf{T} \mathbf{V}_{\boldsymbol{\psi}_3}^{\boldsymbol{\psi}_1 \boldsymbol{\psi}_2} \mathbf{M}_{\boldsymbol{\psi}_1},$$

where \mathbf{M}_{ψ} is defined as before, while $\mathbf{V}_{\psi_3}^{\psi_1\psi_2}$ is a diagonal matrix

$$\left(\mathbf{V}_{\psi_3}^{\psi_1\psi_2}\right)_{ii} = \ell_i^{p(\psi_1,\psi_2,\psi_3)} p_{\psi_3}(\psi_3)_i.$$

Exceptions to the general derivative pattern are listed in Appendix S2. In the previous equation, $p_{\psi}(\psi)_i$ denotes the *i*-th element of the vector

$$p_{\psi}(\psi) = \frac{\mathrm{d}_{\psi}p(\psi)}{\mathrm{d}_{\psi}\rho} = \sum_{l=1}^{K_{\psi}} \left(\mathbf{M}_{\psi}\right)_{.l} \frac{\mathrm{d}\hat{\psi}_{l}}{\mathrm{d}\rho} = \left(\mathbf{M}_{\psi} \frac{\mathrm{d}\hat{\psi}}{\mathrm{d}\rho}\right),$$

where $\frac{d_{\boldsymbol{\psi}}p(\boldsymbol{\psi})}{d_{\boldsymbol{\psi}}\rho}$ is the derivative of $p(\boldsymbol{\psi})$ w.r.t. ρ , when only $\boldsymbol{\psi}$ is function of the log-smoothing parameter, and $(\mathbf{M}_{\boldsymbol{\psi}})_{.l}$ denotes the l-th column of the matrix $\mathbf{M}_{\boldsymbol{\psi}}$.

3.3 Inference and model selection

Adopting the Bayesian view of the smoothing process allows us to quantify the uncertainty of the coefficients ζ . In particular, Wood et al. (2016) employ standard Bayesian asymptotic techniques to approximate the posterior distribution of ζ , $p(\zeta \mid \mathbf{y}, \lambda)$, with a Gaussian centred in the MAP estimate $\hat{\zeta}$ and with covariance $\mathbf{V}_{\zeta} = (\hat{\mathcal{I}} + S_{\lambda})^{-1}$ where $\hat{\mathcal{I}}$ is the Hessian of the negative log-likelihood, i.e., $\zeta \mid \mathbf{y}, \lambda \sim \mathcal{N}(\hat{\zeta}, \mathbf{V}_{\zeta})$. This approximation ignores the uncertainty in the smoothing parameter estimates, which are treated as fixed in the LAML maximiser. In principle, an approximation to the unconditional posterior $p(\zeta \mid \mathbf{y})$ could be obtained by using a Gaussian approximation to $p(\lambda \mid \mathbf{y})$ and then propagating forward the uncertainty of the smoothing parameter. However, the formulas provided by Wood et al. (2016) require the Hessian of $\tilde{\mathcal{V}}(\lambda)$ w.r.t. λ , which involves computing the fourth-order derivative of log-likelihood w.r.t. each element of η . Considering the complexity of the derivative system presented above, we leave this for future work.

Pointwise Bayesian credible intervals for the nested effects can be derived by propagating forward the approximate posterior distribution of ξ via the Delta method. In particular, the asymptotic posterior distribution of a nested effect $s(\tilde{s}(\mathbf{x}))$ can be approximated by using a Gaussian distribution centred at the estimated nested effect $\hat{s}(\hat{s}(\mathbf{x}))$ and with covariance matrix $\mathbf{V}_s = \nabla_{ab}\hat{s}_b \left[\mathbf{V}_{\zeta}\right]_{ab} \left(\nabla_{ab}\hat{s}_b\right)^{\mathsf{T}}$. Here $\left[\mathbf{V}_{\zeta}\right]_{ab}$ indicates the block of \mathbf{V}_{ζ} corresponding to the parameter vectors \mathbf{a} and \mathbf{b} and ∇_{ab} denotes the gradient vector w.r.t. the parameters \mathbf{a} and \mathbf{b} , i.e., $\nabla_{ab}\hat{s}_b = \left[\operatorname{diag}\left(\mathbf{M}_b^1b\right)\mathbf{M}_a,\mathbf{M}_b\right]$.

The Bayesian perspective has also an impact on model selection methods, making it impractical to use marginal likelihood due to the improper priors of smooths. A widely used solution in the regression framework for addressing these challenges is the Akaike's information criterion (AIC). In this work, we adopt the AIC derivation described in Wood et al. (2016) that is easily computed and applicable to the model class considered. More specifically, it is computed as AIC = $-2\ell(\hat{\zeta}) + 2\operatorname{tr}(\mathbf{F})$, where $\operatorname{tr}(\mathbf{F})$ represents the effective degrees of freedom (e.d.f.) and $\mathbf{F} = \mathbf{V}_{\zeta}\hat{\mathcal{I}}$. The e.d.f. of an individual smooth term are obtained by summing up the diagonal elements of \mathbf{F} corresponding to its coefficients. This is a key quantity in measuring the complexity and flexibility of each smooth.

Under the Gaussian additive model assumption, $y = \mu + \varepsilon$ where $\varepsilon \sim \mathcal{N}(0, \sigma^2)$, the above expression for the e.d.f. coincides with the definition proposed by Efron (1986), that is $\hat{\tau} = \sigma^{-1} \operatorname{cov}(\hat{\boldsymbol{\mu}}, \mathbf{y})$. By applying Stein's lemma (Stein, 1981) to the definition, the e.d.f. are expressed as

$$\hat{\tau} = \sum_{i=1}^{n} \frac{\partial \hat{\mu}_i}{\partial y_i} = \sum_{i=1}^{n} \left(\frac{\partial \hat{\mu}_i}{\partial \zeta} \right)^{\top} \frac{\partial \zeta}{\partial y_i}.$$
 (10)

By definition, $\hat{\boldsymbol{\zeta}} = \hat{\boldsymbol{\zeta}}(y)$ satisfies

$$\left. \left(\frac{\partial \ell(y, \zeta)}{\partial \zeta} - \mathbf{S}_{\lambda} \zeta \right) \right|_{\zeta = \hat{\zeta}} = 0,$$

and, by differentiating both sides w.r.t. y, we find

$$\frac{\partial \hat{\boldsymbol{\zeta}}}{\partial y} = -\left(-\frac{\partial^2 \ell(y,\hat{\boldsymbol{\zeta}})}{\partial \boldsymbol{\zeta}^{\top} \partial \boldsymbol{\zeta}} + S_{\boldsymbol{\lambda}}\right)^{-1} \frac{\partial^2 \ell(y,\hat{\boldsymbol{\zeta}})}{\partial \hat{\mu} \partial y} \frac{\partial \hat{\mu}}{\partial \boldsymbol{\zeta}}.$$

Plugging the derivative expression into the definition of $\hat{\tau}$ leads to

$$\hat{\tau} = \sum_{i=1}^{n} \frac{\partial \hat{\mu}_{i}}{\partial \boldsymbol{\zeta}}^{\top} \left(-\frac{\partial^{2} \ell(y, \hat{\boldsymbol{\zeta}})}{\partial \boldsymbol{\zeta}^{\top} \partial \boldsymbol{\zeta}} + S_{\boldsymbol{\lambda}} \right)^{-1} \frac{\partial^{2} \ell(y_{i}, \hat{\boldsymbol{\zeta}})}{\partial \hat{\mu}_{i} \partial y_{i}} \frac{\partial \hat{\mu}_{i}}{\partial \boldsymbol{\zeta}}
= \frac{1}{\sigma^{2}} \operatorname{tr} \left(\left(-\frac{\partial^{2} \ell(y, \hat{\boldsymbol{\zeta}})}{\partial \boldsymbol{\zeta}^{\top} \partial \boldsymbol{\zeta}} + S_{\boldsymbol{\lambda}} \right)^{-1} \sum_{i=1}^{n} \frac{\partial \hat{\mu}_{i}}{\partial \boldsymbol{\zeta}} \frac{\partial \hat{\mu}_{i}}{\partial \boldsymbol{\zeta}}^{\top} \right) = \operatorname{tr} \left(\mathbf{F}_{\hat{\tau}} \right).$$
(11)

Due to the Gaussian assumption $\hat{\mathcal{I}} = \sigma^{-2} \sum_{i=1}^{n} \frac{\partial \hat{\mu}_{i}}{\partial \zeta} \frac{\partial \hat{\mu}_{i}}{\partial \zeta}^{\top}$, which leads to $\hat{\tau}$ being the trace of $\mathbf{F}_{\hat{\tau}} = (\hat{\mathcal{I}} + \mathbf{S}_{\lambda})^{-1} \hat{\mathcal{I}} = \mathbf{V}_{\zeta} \hat{\mathcal{I}} = \mathbf{F}$. Therefore, the general e.d.f. definition based on (10) matches that of Wood et al. (2016), which was based on a different line of reasoning.

4 Applications

Here we illustrate the effectiveness of the nested smooth effects in the context of two challenging applications. Recall that our fitting framework requires the spline bases underlying the nested smooth effects to be four times differentiable. We use B-spline bases of sixth degree (i.e., sextic), which fulfil this requirement and have derivatives that are readily computed via the splines R package. All nested effects are smoothed via second-order derivative penalties. Unless stated otherwise, standard smooth effects are constructed using thin plate spline bases and regularised via second derivative penalties.

4.1 Electricity net-demand in Great Britain

Electricity net-demand is the demand minus embedded generation, measured at the interface between the high-voltage transmission grid and a distribution network. In Great Britain (GB), these interfaces are referred to as Grid Supply Points (GSP) and are organized into 14 regions, known as GSP groups and shown in Figure 3. We are interested in forecasting the total net-demand in GB, that is, its sum across the GSP groups, one day ahead. Such forecasts are key inputs for many operations in the electricity industry, such as trading and production planning. We focus on the net demand between 12:00 AM and 12:30 AM, from January 2014 to December 2018. As predictors, we use calendar information such as bank/school holidays, weekdays, and day of the year, and day-ahead weather forecasts produced by the operational ECMWF-HRES model. The raw weather predictions are available on a spatial grid, but have been reduced to 14 regional forecasts,

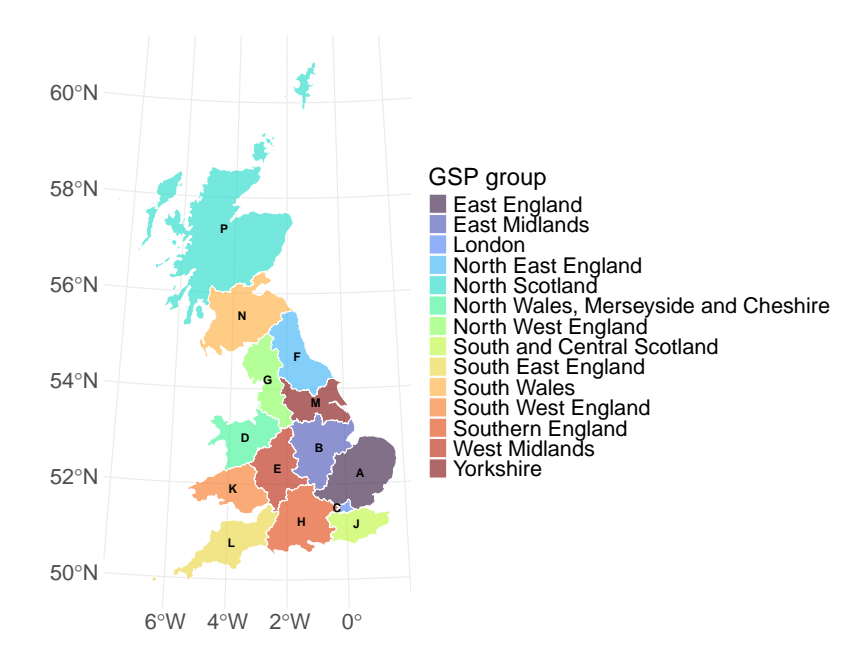


Figure 3: Map of grid supply point groups (GSP) in Great Britain

following the approach of Browell and Fasiolo (2021). The available covariates are listed in Table 1.

Let y_i , i = 1, ..., n be the net-demand, and assume that $y_i \sim \mathcal{N}(\mu_i, \sigma_i^2)$ with mean and variance modelled via

$$\mu_{i} = g_{1}(\mathbf{t}_{i}) + g_{2}(\operatorname{dow}_{i}^{+}) + g_{3}(\operatorname{shol}_{i}) + f_{1}^{30}(\operatorname{doy}_{i}) + f_{2}^{10}(\overline{\operatorname{irr}}_{i}) + f_{3}^{10}(\overline{\operatorname{rain}}_{i}) + s_{1}^{10}(\operatorname{wcap}_{i} \cdot \operatorname{\mathbf{wsp}}_{i}^{\mathsf{T}} \boldsymbol{a}^{w}) + s_{2}^{10}((\mathbf{y}_{i}^{L})^{\mathsf{T}} \boldsymbol{a}^{y}) + s_{3}^{15}(\tilde{s}_{3}^{\exp}(\overline{\operatorname{temp}}_{i})) + s_{4}^{10}(\tilde{s}_{4}^{\exp}(\overline{\operatorname{temp}}_{i}))$$

$$(12)$$

$$\log \sigma_{i}^{2} = g_{4}(\operatorname{st}_{i}) + g_{5}(\operatorname{shol}_{i}) + f_{4}^{10}(\operatorname{doy}_{i}),$$

where g_1 to g_5 are parametric (linear) effects, f_1 to f_4 are standard smooth effects and s_1 to s_4 are smooth effects with nested transformations. The superscripts of the f's and s's indicate the number of spline basis functions used. The spline bases and penalties are those described at the beginning of this section except for $f_1^{30}(\text{doy}_i)$, which uses a B-spline basis with an adaptive P-spline penalty (Eilers and Marx, 1996) designed to allow the smoothness to vary with the covariate (see Section 5.3.5 of Wood, 2017, for details).

The model includes four nested transformations. The first is a linear combination, with single index vector \mathbf{a}^y , of past half-hourly net-demand values \mathbf{y}_i^L , with lags ranging from 12 to 34 hours before y_i is observed. The elements of \mathbf{a}^y are regularised via the second-order difference penalty $\sum_l (a_{l+1}^y - 2a_l^y + a_{l-1}^y)^2$, which encourages them to vary linearly with their index. A further linear combination, with coefficient vector \mathbf{a}^w , is used to reduce the regional wind speed forecasts to a single index, which is then scaled by GB wind generation capacity. We expect its elements to be proportional, in absolute value, to the embedded wind production capacity in each region.

The remaining weather forecasts have been summarised by taking their sample mean across the GSP groups, resulting in the scalar valued covariates $\overline{\text{irr}}_i$, $\overline{\text{rain}}_i$ and $\overline{\text{temp}}_i$. To justify this choice, note that $\overline{\text{irr}}_{ij}$ is already scaled by the installed solar production

Gene	eral covariates	Covariates derived from weather forecasts				
$\operatorname{dow}_{i}^{+}$	day of the week factor with additional factor levels accounting for public holidays	$ \operatorname{rain}_{ij} \operatorname{squared} \operatorname{root} \operatorname{mean} \operatorname{precipitation} (\sqrt{mm \ h^{-1}}) $				
\mathbf{t}_i	time since the 1st January 2014	$\operatorname{temp}_{ij}\operatorname{temperature}$ (K) at cell with highest regional population density				
wcap	$_{i}\mathrm{GB}$ embedded wind generation capacity (MW)	irr _{ij} squared root mean solar irradiance $(\sqrt{W} \ m^{-2})$ times embedded solar generation capacity (MW)				
doy_i	day of the year $(\in \{1, \dots, 366\})$	$\operatorname{wsp}_{ij}^{100}$ squared root mean wind speed at 100 metres $(\sqrt{m~s^{-1}})$				
shol_i	school holidays, three levels factor to distinguish Christmas from other holidays					
y_i^h	net-demand at h hours lag					
st_i	factor denoting the presence of a storm in GB					

Table 1: Variables used to model net-demand in Great Britain. The subscript i indicates the i-th observation, and j denotes the j-th GSP group.

capacity in the j-th region, so estimating regional weights, as we did for wind speed, seems unnecessary. During model development, we experimented with single index effects for precipitation and temperature, but the estimated weights did not vary significantly across the regions. Hence, we opted for standard smooth effects of their mean values across GB.

The third and fourth nested effects in (12) are based on exponential smooth effects of average GB temperature. Such effects are meant to capture thermal inertia, which might evolve at an intra-day scale. However, we are forecasting only one value of y_i per day, hence the effects must handle different temporal resolutions. In particular, exponential smoothing is performed on a half-hourly resolution, that is $\tilde{s}_{3-4}^{\text{exp}}(\overline{\text{temp}}_i)$ use the $48 \times i$ temperature forecasts that are available before the *i*-th net-demand value is observed, but only the smoothed temperature value corresponding to 12 AM is used to predict y_i . The irregular time gaps induced by missing temperature values are handled by letting the exponential smoothing rate vary with $\tilde{\mathbf{x}}_i^{\mathsf{T}} \mathbf{a}^{\mathrm{exp}}$, where $\tilde{\mathbf{x}}_i = [1, \Delta h_i - 1]$ and Δh_i is the number of hours between $\overline{\mathrm{temp}}_i$ and the preceding temperature forecast.

We fitted model (12) on data from 2014 to 2017, leaving 2018 for testing. Figure 4 shows some of the estimated effects and inner transformations. The top row shows the linear combination coefficients of wind speed (left) and the corresponding smooth effect (right). As expected, the single index elements that are significantly different from zero correspond to GSP groups with substantial wind production capacity, namely North Wales and Merseyside (D), South and Central Scotland (N), and North Scotland (P). Considering that the smooth effect of wind speed is monotonically decreasing, this suggests that, as wind speed increases, net-demand decreases due to the growth in embedded wind production. In contrast, the coefficient for London (C) is negative, hence net-demand increases with wind speed in this region. Even though the coefficient is not significantly different from zero and should not be over-interpreted, its sign is more likely to be related to the cooling effect of wind speed, rather than to wind production, which is negligible in this highly urbanised

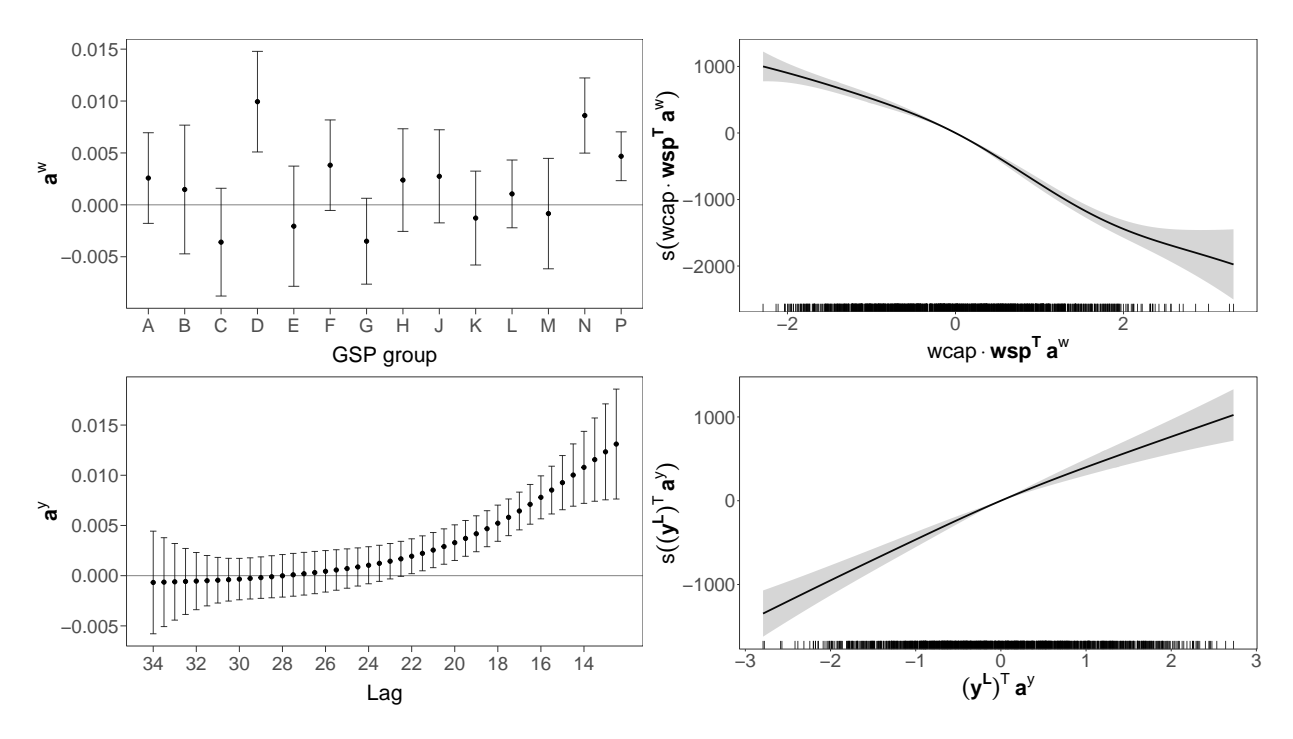


Figure 4: Inner single index coefficients and outer smooth effect of wind speed (top) and of net-demand lags (bottom).

area.

The bottom row of Figure 4 shows the single index coefficients of lagged net-demand (left) and the corresponding effect (right). In accordance with intuition, the overall effect of lagged demand is positive, as all the non-zero coefficients are positive and the smooth effect is monotonically increasing. Further, the coefficients decrease monotonically as the lag increases, meaning that recent net-demand values are more informative for predicting future net-demand. Note that this was not obvious a priori, because net-demand behaves differently depending on the hour of the day. In particular, here the most recent lag, which corresponds to 11:30 PM, has been assigned the highest weight when predicting net-demand at 12 AM.

The exponentially smoothed temperatures and their effect on net-demand are shown on the top row of Figure 1. The two effects converged on different smoothing regimes, corresponding to exponential parameters approximately equal to 0.5 (red) and 0.995 (blue). The red smoothed temperature trajectory corresponds to a low thermal inertia regime. It affects net-demand via a U-shaped effect, which arguably captures both heating and cooling. Instead, the blue temperature trajectory, is characterised by higher inertia, and it affects net-demand only via cooling. This could be due to the fact that heat-waves are usually of short duration in GB, hence they are effectively filtered out by the smoother temperature trajectory.

To validate the model, we compare its predictive performance with that of four alternative models on the 2018 test data. All such models assume a Gaussian response and model $\log \sigma_i^2$ as in (12). Their mean parameter is controlled by the effects appearing on the first row of (12), that is from g_1 up to f_3 (omitted below), but the remaining effects have been

	Log-score	CRPS	RMSE	MAE	AIC	Time (s)
M1	2671.238	133820.1	720.1707	560.9411	21668.85	43
M2	2667.346	129073.0	692.4466	537.6058	21550.47	44
M3	2659.871	125553.5	673.1477	524.4006	21499.80	47
M4	2630.694	115332.6	634.9627	476.8524	21297.01	50441
Model (12)	2635.993	114061.8	622.3888	470.9798	21265.87	734

Table 2: Comparison of out-of-sample performance in the electricity net-demand application, using nested versus standard effects.

replaced with the following

$$\mu_i^1 = \dots + f_4^{15}(\overline{\text{temp}}_i) + f_5^{10}(\overline{\text{wind}}_i) + f_6(y_i^{24}),$$
 (M1)

$$\mu_i^2 = \dots + f_4^{15}(\overline{\text{temp}}_i) + f_5^{10}(\overline{\text{wind}}_i) + f_6^{25}(\mathbf{y}_i^L),$$
 (M2)

$$\mu_i^3 = \dots + f_4^{15}(\overline{\text{temp}}_i) + f_5^{10}(\overline{\text{wind}}_i) + f_6^{25}(\mathbf{y}_i^L) + f_8^{10}(\overline{\text{temp}}_i^{95}),$$
 (M3)

$$\mu_i^4 = \dots + f_4^{15}(\overline{\text{temp}}_i) + f_5^{10}(\overline{\text{wind}}_i) + f_6^{25}(\mathbf{y}_i^L) + f_8^{10}(\overline{\text{temp}}_i^{95}) + s_5^{10}(\text{wcap}_i \cdot \mathbf{wsp}_i^\mathsf{T} \boldsymbol{a}^{wsp}).$$
(M4)

Here $\overline{\text{wind}}_i$ is the sample mean of wind speeds across the GSP groups and $f_6^{10}(\mathbf{y}_i^L)$ is a distributed lag effect. The latter is a type of functional smooth effect obtained by building a bi-variate tensor-product smooth effect of lagged net-demand and the corresponding lag, which is then integrated over the lag. It is an obvious alternative to the single index effect of lagged demand, that is effect s_2 in (12). A simpler alternative is provided by M1, which includes the effect of net-demand at a 24-hour lag only. Variable $\overline{\text{temp}}_i^{95}$ is an exponential smooth of the average GB temperature with smoothing coefficient fixed a priori to 0.95, which is a commonly used value in aggregate demand forecasting applications (see, e.g., Gaillard et al., 2016). The last effect in M4 is a single index effect of wind speed, where the index coefficients have been estimated by maximising the profile LAML in an outer iteration, which requires refitting the model multiple times, rather than via the methods proposed here.

The first three columns of Table 2 report the performance of each model in terms of out-of-sample negative log-likelihood (log-score), marginal continuous ranked probability score (CRPS) and root mean squared error (RMSE). The table shows a clear improvement in performance as model complexity increases from M1 to M4, with model (12) leading to the lowest losses. The AIC of each model in the fourth column are in accordance with the out-of-sample losses. The last column reports the fitting times, and show that the proposed model is around twenty times slower than standard GAMs with no nested effects (M1-M3).

4.2 Modelling house prices in London

Here we focus on modelling how house prices are affected by local socio-economical factors, as well as by characteristics of the property being sold, while accounting for spatial autocorrelation. We consider publicly available price paid data in London during 2022, provided by HM Land Registry. In addition to sales prices and the corresponding postcodes, the data contains several categorical variables providing information on each property, specifically:

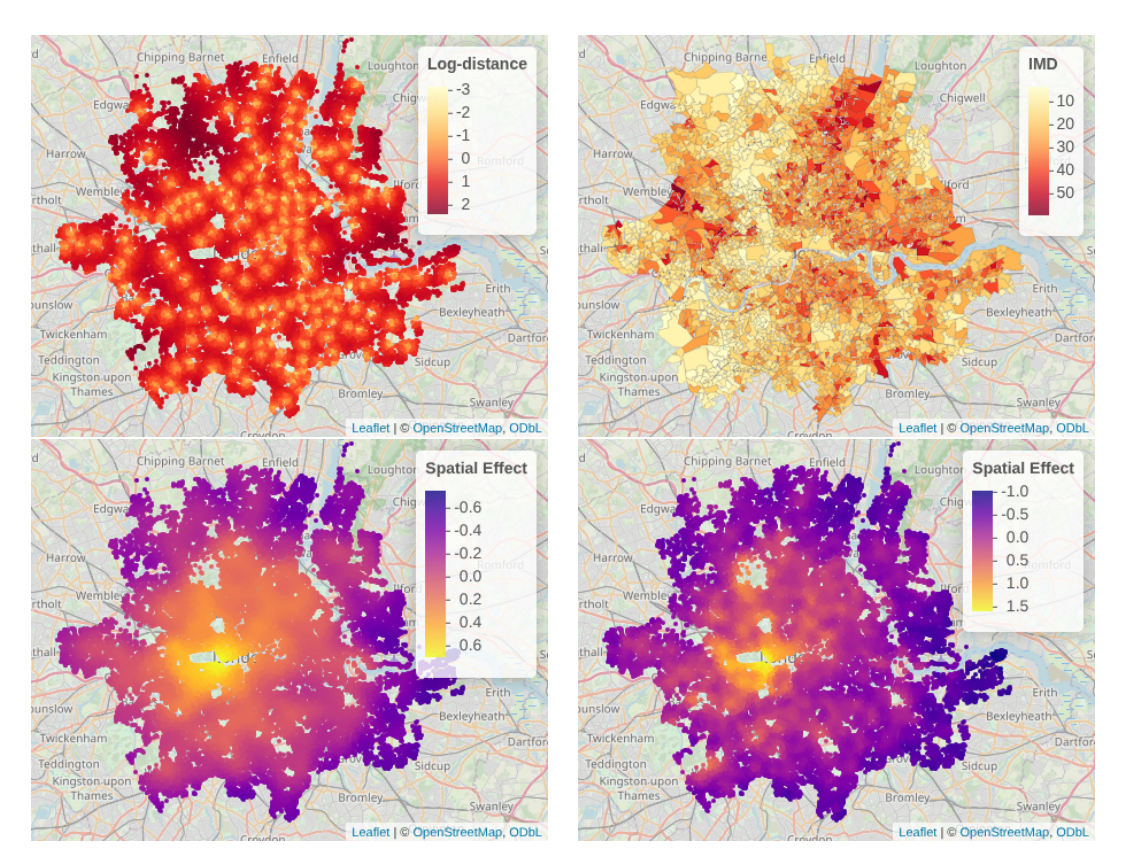


Figure 5: Logarithmic distance of each sold property from the closest underground station (top left), Index of Multiple Deprivation for each LSOA in London (top right), estimated spatial effect under the nested model (13) (bottom left) and under a standard model, with k = 2000 (bottom right).

property type, type_i (detached, semi-detached, terraced, flats/maisonettes or other), the age of the property, new_i (newly built or established residential building), type of price paid, cat_i (standard or additional), and type of ownership, free_i (freehold or leasehold). We integrate the data with the Index of Multiple Deprivation (IMD), which is a composite measure relative deprivation. The index is provided on small areas, comprising between 400 and 1200 households, called Lower layer Super Output Areas (LSOAs), and it is shown on the top right of Figure 5. Further, we compute the Euclidean log-distance, d_i , of each property from the nearest underground station, shown on the top left of Figure 5. See Appendix S6 for more details on data sources.

The full data set comprises 69201 sales, reduced to 67686 after excluding properties sold for less than £100,000 or more than £10 million. We exclude extremely low or high transactions prices because they might be heavily affected by exceptional circumstances, hence entirely unrelated to factors of interest, such as the distance from the tube (the highest price in the full data is £429 million). Further, postcodes are highly localised in the UK, for example a large block of flats can be attributed a unique postcode, leading to highly correlated postcode-level prices. Hence, we average prices at postcode level, thus obtaining a data set of 34537 observed prices.

Let y_i be the logarithm of the averaged price in postcode i. We model its conditional distribution using a GAMLSS model based on the sinh-arcsinh distribution of Jones and

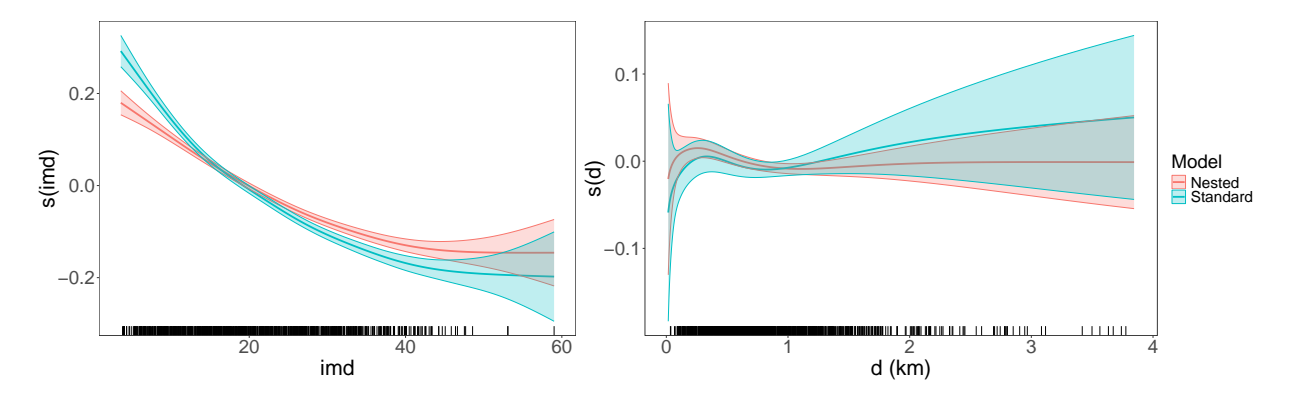


Figure 6: Effects of IMD (left) and distance to the nearest tube station (right), estimated by model (13) and a model using k = 2000 basis functions for the standard spatial effect, but no autoregressive effect.

Pewsey (2009), which has four parameters μ , $\sigma > 0$, ϵ , and $\delta > 0$, controlling location, scale, skewness, and kurtosis. The model allows for asymmetry to either side, depending on the sign of ϵ , and can have lighter tails ($\delta > 1$) or heavier ($0 < \delta < 1$) than a Gaussian distribution. We model ϵ and δ only via intercepts, while the location and scale parameters are controlled by

$$\mu_{i} = g_{1}(\text{type}_{i}) + g_{2}(\text{new}_{i}) + g_{3}(\text{free}_{i}) + g_{4}(\text{cat}_{i}) + f_{1}^{10}(\text{imd}_{i}) + f_{2}^{10}(\text{d}_{i}) + f_{3}^{400}(\text{lon}_{i}, \text{lat}_{i}) + s^{10}(\tilde{s}^{\text{mgks}}(\tilde{\mathbf{x}}_{i}))$$

$$\log(\sigma_{i}^{2}) = g_{5}(\text{type}_{i}) + g_{6}(\text{cat}_{i}) + f_{4}^{10}(\text{imd}_{i}).$$
(13)

As in the net-demand application, the g's indicate parametric effects and the f's standard smooth effects. The latter are based on the spline bases and penalties described at the beginning of this section, including f_3 , which is an isotropic bivariate spatial effect.

The last smooth effect used to model μ_i in (13) contains a nested bivariate Gaussian kernel smoothing transformation of neighbouring house log-prices. In particular

$$\tilde{s}(\mathbf{x}_i) = \frac{\sum_{j \in \mathcal{N}_i} K_a(\mathbf{x}_i, \mathbf{x}_j) y_j}{\sum_{a \in \mathcal{N}_i} K_a(\mathbf{x}_i, \mathbf{x}_q)},$$
(14)

where $\mathbf{x}_i = \{ \text{lon}_i, \text{lat}_i \}$, \mathcal{N}_i is the set of the L postcodes that are closest to i in Euclidean distance, K_i is the bivariate Gaussian p.d.f with diagonal, isotropic covariance matrix, parametrised by a. The purpose of this smooth is to capture the effect of neighbouring prices via a spatial autoregressive model, where the rate of decay of the spatial weights is controlled by a. Here we use L = 25 neighbours to reduce the computational cost, but the results below are unchanged by setting L = 100.

To quantify the importance of including the spatial autoregressive component in (13), we consider a sequence of models that do not include such an effect. In particular, we remove the autoregressive term and we fit models that only use $f_3^k(\text{lon}_i, \text{lat}_i)$, with different basis dimension k, to model the spatial variation of house log-prices. We test the model on a test set, generated by random splitting the postcodes between a train (75% of the data) and a testing set (25%).

The results on the same loss functions considered in Section 4.1 are shown in Table 3. The second column reports the number of basis functions, k, used for the isotropic spatial

	Knots	Log-score	CRPS	RMSE	MAE	AIC	Time (min)
standard	400	3899	1949	0.437	0.304	23029	40
standard	1000	3807	1925	0.433	0.301	22105	194
standard	1600	3777	1915	0.432	0.299	21779	444
standard	2000	3771	1915	0.431	0.299	21715	1533
nested	400	3690	1895	0.427	0.297	21653	84

Table 3: Comparison of out-of-sample performance in the house prices modelling application, using nested versus standard spatial effects, with varying basis dimensions.

effect in each model. It is interesting to note that achieving a predictive performance similar to that of the autoregressive models requires a highly parametrised spatial effect (k = 2000), which results in a computational time that is nearly twenty times longer.

The bottom row of Figure 5 shows the estimated spatial effect $f_3^k(\log_i, \log_i)$ under model (14) on the right, and a standard model that uses k = 2000 basis functions on the left. The plots demonstrate that removing the autoregressive term leads to a spatial effect that is both more complex and stronger (note that the colour scale is wider on the right). Arguably, the nested model is more interpretable as it separates the short-range autoregressive process shown on the bottom left of Figure 1 from the smoother spatial effect shown in Figure 5. Instead, long- and short-range price dynamics are confounded in the standard model.

The plot on the bottom right of Figure 1 shows the effect of the kernel-smoothed logprices (bottom left) on μ_i , hence on the expected value of y_i . Interestingly, the slope of the effect increases with the neighbouring prices, suggesting that the autoregressive effect is stronger on the upper end of the price range. Note that the median price is around 600£ thousand, or $y \approx 13.3$ on the log-scale.

The effect of IMD and distance from the tube, estimated under model (14) and the standard model with k = 2000, are shown in Figure 6. As expected, prices are inversely proportional to IMD, with a slightly stronger effect under the standard model. The effect of distance from the tube is weaker, with model (14) estimating a slight decrease in prices with distance. Interestingly, the effect flattens beyond one kilometre, which is coherent with recent studies (BBC News, 2025).

5 Conclusion

This work introduces a novel framework for incorporating complex covariate transformations into multi-parameter GAMs, with particular emphasis on transformations that provide automatic feature-engineering capabilities. By extending the implicit differentiation methods of Wood et al. (2016) to accommodate the structure of nested effects, we enable the joint estimation of regression coefficients and transformation parameters. Doing so removes the need for a separate data preprocessing step, as well as the costly re-fitting of the entire model to determine transformation coefficients. Additionally, it enables joint uncertainty quantification of all parameters through approximate Bayesian methods.

Motivated by applications in electricity net-demand forecasting and house-price modelling, we focus on three specific types of interpretable transformations designed to handle complex covariates, such as time-series and spatial data. However, the modular fitting and inferential framework developed here is sufficiently general to incorporate any scalarvalued function \tilde{s} that is sufficiently differentiable w.r.t. its parameters, thus providing several directions for future research. For example, it would be interesting to consider single index effects where the inner coefficients are constrained, as done by Masselot et al. (2022). Doing so would enhance the interpretability of the results, especially when the linear transformation is viewed as an index or a weighted average.

Finally, it is worth noting that the proposed framework would, in principle, permit the inclusion of composite transformations obtained by nesting several basic transformations. Incorporating such transformations into multi-parameter GAMs would bring them closer to deep learning models with embedded feature engineering capabilities, while still preserving the interpretability associated with an additive structure. This interpretability is crucial in high-stakes applications, such as net-demand forecasting for power-production planning, where understanding the rationale behind a model is essential.

Acknowledgments

Claudia Collarin's work has been partially funded by PON "Research and Innovation" 2014–2020 Action IV.5 "PhDs on Green issues." – Ministerial Decree 1061/2021. Matteo Fasiolo's work has been partially funded by EDF R&D. This work contains HM Land Registry data © Crown copyright and database right 2021. This data is licensed under the Open Government Licence v3.0.

References

- Antoniadis, A., G. Grégoire, and I. W. McKeague (2004). Bayesian estimation in single-index models. *Statistica Sinica* 14(4), 1147–1164.
- BBC News (2025, Nov). Londoners 'pay £43k premium to live near rail line'. Accessed: 2025-11-20.
- Box, G. E. P. and D. R. Cox (1964). An analysis of transformations. *Journal of the Royal Statistical Society: Series B (Methodological)* 26(2), 211–243.
- Browell, J. and M. Fasiolo (2021). Probabilistic forecasting of regional net-load with conditional extremes and gridded nwp. *IEEE Transactions on Smart Grid* 12(6), 5011–5019.
- Carroll, R. J., J. Fan, I. Gijbels, and M. P. Wand (1997). Generalized partially linear single-index models. *Journal of the American Statistical Association* 92(438), 477–489.
- Collins, G., D. Francom, and K. Rumsey (2024). Bayesian projection pursuit regression. Statistics and Computing 34(1), 29.
- Efron, B. (1986). How biased is the apparent error rate of a prediction rule? *Journal of the American Statistical Association* 81(394), 461–470.
- Eilers, P. H. and B. D. Marx (1996). Flexible smoothing with b-splines and penalties. Statistical Science 11(2), 89–121.

- Fan, C., and J. P. Fine (2013). Linear transformation model with parametric covariate transformations. *Journal of the American Statistical Association* 108(502), 701–712.
- Fischer, M., R. Füss, and S. Stehle (2018). Spillover effects in residential house prices.
- Friedman, J. H. and W. Stuetzle (1981). Projection pursuit regression. *Journal of the American statistical Association* 76(376), 817–823.
- Gaillard, P., Y. Goude, and R. Nedellec (2016). Additive models and robust aggregation for gefcom2014 probabilistic electric load and electricity price forecasting. *International Journal of Forecasting* 32(3), 1038–1050.
- Gasparrini, A., F. Scheipl, B. Armstrong, and M. G. Kenward (2017). A penalized framework for distributed lag non-linear models. *Biometrics* 73(3), 938–948.
- Greven, S. and F. Scheipl (2017). A general framework for functional regression modelling. *Statistical Modelling* 17(1-2), 1–35.
- Guerrieri, V., D. Hartley, and E. Hurst (2013). Endogenous gentrification and housing price dynamics. *Journal of Public Economics* 100, 45–60.
- Jones, M. and A. Pewsey (2009). Sinh-arcsinh distributions. *Biometrika* 96(4), 761–780.
- Kabán, A. (2012). Non-parametric detection of meaningless distances in high dimensional data. Statistics and Computing 22(2), 375–385.
- Kallberg, J. G. and Y. Shimizu (2025, January). Crime measures and housing prices: an analysis using quantile regression and spatial autocorrelation. *The Journal of Real Estate Finance and Economics*.
- LeSage, J. and R. K. Pace (2009). *Introduction to spatial econometrics*. Chapman and Hall/CRC.
- Liang, H., X. Liu, R. Li, and C.-L. Tsai (2010). Estimation and testing for partially linear single-indexmodels. *Annals of statistics* 38(6), 3811–3836.
- Lindgren, F., H. Rue, and J. Lindström (2011). An explicit link between gaussian fields and gaussian markov random fields: the stochastic partial differential equation approach. Journal of the Royal Statistical Society Series B: Statistical Methodology 73(4), 423–498.
- Masselot, P., F. Chebana, C. Campagna, E. Lavigne, T. B. M. J. Ouarda, and P. Gosselin (2022). Constrained groupwise additive index models. *Biostatistics* 24(4), 1066–1084.
- McLean, M. W., G. Hooker, A.-M. Staicu, F. Scheipl, and D. Ruppert (2014). Functional generalized additive models. *Journal of Computational and Graphical Statistics* 23(1), 249–269.
- Muggeo, V. M. R. (2008). Modeling temperature effects on mortality: multiple segmented relationships with common break points. *Biostatistics* 9(4), 613–620.
- Pya, N. and S. N. Wood (2015). Shape constrained additive models. *Statistics and Computing* 25(3), 543–559.

- Rigby, R. A. and D. M. Stasinopoulos (2005). Generalized additive models for location, scale and shape. *Journal of the Royal Statistical Society: Series C (Applied Statistics)* 54(3), 507–554.
- Rue, H., S. Martino, and N. Chopin (2009). Approximate bayesian inference for latent gaussian models by using integrated nested laplace approximations. *Journal of the Royal Statistical Society Series B: Statistical Methodology* 71(2), 319–392.
- Stein, C. M. (1981). Estimation of the mean of a multivariate normal distribution. *The Annals of Statistics* 9(6), 1135–1151.
- Thompson, W. K. (2003). Transformations of covariates for longitudinal data. *Biostatistics* 4(3), 353–364.
- Verdonck, T., B. Baesens, M. Óskarsdóttir, and S. vanden Broucke (2024). Special issue on feature engineering editorial. *Machine learning* 113(7), 3917–3928.
- Wolkowicz, H. and G. Styan (1979). Extensions of Samuelson's inequality. *American Statistician AMER STATIST 33*, 143–144.
- Wood, S. N. (2017). Generalized Additive Models: An Introduction with R. (2 ed.). Boca Raton, FL, USA: Chapman & Hall/CRC.
- Wood, S. N., N. Pya, and B. Säfken (2016). Smoothing parameter and model selection for general smooth models. *Journal of the American Statistical Association* 111(516), 1548–1563.
- Yu, Y., C. Wu, and Y. Zhang (2017). Penalised spline estimation for generalised partially linear single-index models. *Statistics and Computing* 27(2), 571–582.
- Zanobetti, A., M. P. Wand, J. Schwartz, and L. M. Ryan (2000). Generalized additive distributed lag models: quantifying mortality displacement. *Biostatistics* 1(3), 279–292.

Supplementary material to "Integrating Complex Covariate Transformations in Generalized Additive Models"

Claudia Collarin, Matteo Fasiolo, Yannig Goude, Simon N. Wood

S1 Practical details on the solution to the scaling issue

In Section 2.3, we presented the scaling and knots placement issues encountered in the development of nested effects, and we briefly described the proposed solution. The aim of this section is to provide practical details on how to implement the constraints on sample mean and variance.

The straightforward extension of rescaling the norm of \boldsymbol{a} to a general transformation $\tilde{s}(\mathbf{x})$ is

$$\tilde{s}'(\mathbf{x}) = Z(\tilde{s}(\mathbf{x})) = \frac{\tilde{s}(\mathbf{x}) - \bar{\tilde{s}}(\mathbf{x})}{\sqrt{\hat{var}[\tilde{s}(\mathbf{x})]}},$$
 (S1)

where $Z(\cdot)$ denotes the centring and scaling of $\tilde{s}(\mathbf{x})$ by its sample mean and standard deviation. Such a standardisation step can be easily integrated in nested smooth effects. However, note that standardising the transformation can lead to identifiability problems. This is easily seen within the linear transformation case. In this context, standardisation means applying two constraints: a zero mean and a unit norm. Therefore, if p represents the dimension of the vector \boldsymbol{a} of the linear combination coefficients, then the space containing \boldsymbol{a} is actually (p-2)-dimensional. To avoid identifiability issues, two parameters must be removed from \boldsymbol{a} . For the specific single index case, standardisation can be achieved via simple reparametrisation. This process involves centring to zero by subtracting the sample mean from each column in \mathbf{x} . The variance constraint, vâr $(\boldsymbol{a}^{\mathsf{T}}\mathbf{x}) = c$, is achieved by expressing \boldsymbol{a} as a linear transformation of a unit norm vector $\boldsymbol{\omega}$, i.e. $||\boldsymbol{\omega}|| = 1$. Indeed, denote as $\hat{\boldsymbol{\Sigma}}$ the empirical covariance matrix of $\mathbf{x}_1, \ldots, \mathbf{x}_n$. Then $\boldsymbol{a} = \sqrt{c}\mathbf{Q}\boldsymbol{\Lambda}^{-1/2}\boldsymbol{\omega}$, where $\hat{\boldsymbol{\Sigma}} = \mathbf{Q}\boldsymbol{\Lambda}\mathbf{Q}^{\mathsf{T}}$ and the variance of the linear transformation is then equal to c:

$$\hat{\text{var}}(\boldsymbol{a}^{\mathsf{T}}\mathbf{x}) = \boldsymbol{a}^{\mathsf{T}}\hat{\boldsymbol{\Sigma}}\boldsymbol{a} = c\boldsymbol{\omega}^{\mathsf{T}}\boldsymbol{\Lambda}^{-1/2}\mathbf{Q}^{\mathsf{T}}\mathbf{Q}\boldsymbol{\Lambda}\mathbf{Q}^{\mathsf{T}}\mathbf{Q}\boldsymbol{\Lambda}^{-1/2}\boldsymbol{\omega} = c.$$

Although this parametrisation bypasses the scaling problem mentioned earlier in this section, it spoils the linearity of the transformation with respect to its parameters. This fact has significant implications: It loses the computational benefits (discussed in Section 3.2) inherent in the linear combination and affects the interpretability of the results due to rotation and scaling via $\sqrt{c}\mathbf{Q}\mathbf{\Lambda}^{-1/2}$. Therefore, to avoid identifiability issues and to preserve the linearity of the effect with respect to the parameters, we adopt a penalty-based approach.

Specifically, define the centred and scaled transformation

$$\tilde{s}'(\mathbf{x}) = e^{a_0}(\tilde{s}(\mathbf{x}) - \bar{\tilde{s}}(\mathbf{x})),$$
 (S2)

where the additional parameter $a_0 \in \mathbb{R}$ controls the scale of the transformation. Then, the constraint on the variance is imposed by including the penalty term $q_{\tilde{s}'} = (\hat{var}[\tilde{s}'(\mathbf{x})] - c)^2$ to (6) leading to:

$$\mathcal{L}(\boldsymbol{\zeta}) = \log p(\boldsymbol{\zeta}|\boldsymbol{y}, \boldsymbol{\lambda}) = \sum_{i=1}^{n} \ell_i(\boldsymbol{\zeta} \mid y_i) - \frac{1}{2} \sum_{g=1}^{G} \lambda_g \boldsymbol{\zeta}^\mathsf{T} \mathbf{S}_g \boldsymbol{\zeta} - \sum_{u=1}^{U} q_u(\boldsymbol{\zeta}), \tag{S3}$$

where U denotes the total number of nested effects in the model. Note that while the constraint on $v\hat{a}r(\tilde{s}'(\mathbf{x}))$ is imposed on all elements of \mathbf{a} , in practice only a_0 is affected by it. This is because, in the absence of this constraint, a_0 would be very weakly identifiable. To see this, consider the case where $s(\tilde{s}'(\mathbf{x}))$ is constructed via a polynomial basis, that is, $s(\tilde{s}'(\mathbf{x})) = \tilde{s}'(\mathbf{x})b_1 + (\tilde{s}'(\mathbf{x}))^2b_2 + \cdots + (\tilde{s}'(\mathbf{x}))^Lb_L$. Plugging in $\tilde{s}'(\mathbf{x}) = a_0\tilde{s}(\mathbf{x})$ shows that each power of a_0 can be absorbed into the corresponding b_l without changing $s(\tilde{s}'(\mathbf{x}))$. For most other complex basis, the lack of identifiability is less than perfect but it is, in our experience, strong enough to lead to divergence during model fitting, if a constraint is not applied.

Interestingly, the unidentifiability of a_0 is an advantage in our context, because it allows us to satisfy the constraint $var[\tilde{s}'(\mathbf{x})] = c$ almost exactly by penalising $q_{\tilde{s}'}$, rather than reparametrising a so that the constraint is exactly met. Such a reparametrisation would be very cumbersome, because it would need to be analytically derived for each type of transformation, thus slowing down the development of new models. Instead, the penalty-based alternative is agnostic to the type of transformation used, and it is easily integrated into the model fitting framework adopted here.

The addition of a_0 to \boldsymbol{a} and the centring are not necessary for the linear combinations described in Section 2.2.3. In fact, the linear transformation is centred around 0 by subtracting from each column in \mathbf{x}_i its mean, while the scale of $\tilde{s}(\mathbf{x}_i)$ is implicity controlled by $||\boldsymbol{a}||$. Hence, adding a further scale parameter a_0 is unnecessary and $||\boldsymbol{a}||$ is determined by the penalty mentioned. Finally, note that the sign of \boldsymbol{a} is not identifiable. This is not a problem for model fitting, but some care is needed when interpreting the model output.

S2 Exceptions to the derivatives of Hessian blocks

In Section 3, the smoothing parameters λ have been selected by maximising a Laplace approximate marginal likelihood (Equation 7, LAML). Using the same notation as in Section 3.2, we provide the derivatives of Hessian blocks that do not follow the pattern $\Gamma_3^{12} = \mathbf{M}_{\psi_2}^{\mathsf{T}} \mathbf{V}_{\psi_3}^{\psi_1 \psi_2} \mathbf{M}_{\psi_1}$. Recall that

$$p(\boldsymbol{\psi}) = \begin{cases} \eta & \boldsymbol{\psi} \in \{\boldsymbol{\gamma}_{l}, \boldsymbol{\beta}_{u}, \boldsymbol{b}_{u}\} \\ \tilde{s}_{\boldsymbol{\psi}} & \boldsymbol{\psi} \in \{\boldsymbol{\alpha}_{u}, \boldsymbol{a}_{u}\} \end{cases}$$
$$p_{\boldsymbol{\psi}}(\boldsymbol{\psi}) = \frac{\mathrm{d}_{\boldsymbol{\psi}}p(\boldsymbol{\psi})}{\mathrm{d}_{\boldsymbol{\psi}}\rho} = \mathbf{M}_{\boldsymbol{\psi}} \frac{\mathrm{d}\hat{\boldsymbol{\psi}}}{\mathrm{d}\rho} = \begin{cases} \mathbf{M}_{\boldsymbol{\psi}} \frac{\mathrm{d}\hat{\boldsymbol{\psi}}}{\mathrm{d}\rho} & \boldsymbol{\psi} \in \{\boldsymbol{\gamma}_{l}, \boldsymbol{\beta}_{u}, \boldsymbol{b}_{u}\} \\ \nabla_{\boldsymbol{\psi}}\tilde{s}_{\boldsymbol{\psi}} \frac{\mathrm{d}\hat{\boldsymbol{\psi}}}{\mathrm{d}\rho} & \boldsymbol{\psi} \in \{\boldsymbol{\alpha}_{u}, \boldsymbol{a}_{u}\} \end{cases}.$$

Here the sets $\{\gamma_l, \beta_u, b_u\}$ and $\psi \in \{\alpha_u, a_u\}$ represent all vectors in model (1) with a similar meaning (e.g. regression coefficients of both non nested and nested effects, inner coefficients). Greek letters indicate nested effects where the inner transformation is a linear combination. Denoting the differentiation order as $t = 1, 2, \ldots$, define

$$\mathbf{M}_{m{\psi}}^t = egin{cases} rac{\partial^t \mathbf{M}_{m{\psi}}}{\partial m{ ilde{s}}^t} & m{\psi} \in \{m{eta}_u, m{b}_u\} \
abla^t_{m{\psi}} \mathbf{M}_{m{\psi}} = \underbrace{rac{\partial^t \mathbf{M}_{m{\psi}}}{\partial m{\psi} \cdots \partial m{\psi}}}_{t \ times} & m{\psi} \in \{m{lpha}_u, m{a}_u\} \ .$$

Note that in the second row, $\nabla_{\boldsymbol{\psi}}^t \mathbf{M}_{\boldsymbol{\psi}} = \nabla_{\boldsymbol{\psi}}^{t+1} \tilde{\boldsymbol{s}}_{\boldsymbol{\psi}}$ is a tensor of order t+2 whose first dimension is equal to the number of observations. For any $\boldsymbol{\psi} \in \{\boldsymbol{\beta}_u, \boldsymbol{b}_u\}$, define $p_{\boldsymbol{\psi}}^t(\boldsymbol{\psi}) = \mathbf{M}_{\boldsymbol{\psi}}^t \frac{\mathrm{d}\hat{\boldsymbol{\psi}}}{\mathrm{d}\rho}$. In

the specific case where $\psi \in \{\alpha_u, a_u\}$, $p_{\psi}^t(\psi)$ is a tensor. Thus, multiplication by a vector contracts the tensor along its last index. To stress this fact, denote it by the capital letter $\mathbf{P}_{\psi}^t = \sum_{k=1}^p [\mathbf{M}_{\psi}^t]_{\cdot k} \frac{\mathrm{d}\hat{\psi}_k}{\mathrm{d}\rho}$. Then, the exceptional blocks are:

• $\Gamma_{\beta}^{\alpha\alpha}$, where the diagonal matrix has two additional terms

$$(\mathbf{V}_{\boldsymbol{\beta}}^{\boldsymbol{\alpha}\boldsymbol{\alpha}})_{ii} = \ell_i^{p(\boldsymbol{\alpha},\boldsymbol{\alpha},\boldsymbol{\beta})} p_{\boldsymbol{\beta}}(\boldsymbol{\beta})_i + 2\ell_i^{p(\boldsymbol{\alpha},\boldsymbol{\beta})} p_{\boldsymbol{\beta}}^1(\boldsymbol{\beta})_i + \ell_i^{p(\boldsymbol{\beta})} p_{\boldsymbol{\beta}}^2(\boldsymbol{\beta})_i.$$

• $\Gamma_{\alpha}^{\beta\beta}$ (and Γ_{a}^{bb}) have two additional terms

$$\boldsymbol{\Gamma}_{\alpha}^{\beta\beta} = \left(\boldsymbol{M}_{\beta}\right)^{\mathsf{T}} \boldsymbol{V}_{\alpha 1}^{\beta\beta} \boldsymbol{M}_{\beta} + \left(\boldsymbol{M}_{\beta}^{1}\right)^{\mathsf{T}} \boldsymbol{V}_{\alpha 2}^{\beta\beta} \boldsymbol{M}_{\beta} + \left(\left(\boldsymbol{M}_{\beta}^{1}\right)^{\mathsf{T}} \boldsymbol{V}_{\alpha 2}^{\beta\beta} \boldsymbol{M}_{\beta}\right)^{\mathsf{T}},$$

where

$$\left(\mathbf{V}_{\alpha 1}^{\beta \beta}\right)_{ii} = \ell_i^{p(\beta,\beta,\alpha)} p_{\alpha}(\alpha)_i, \qquad \left(\mathbf{V}_{\alpha 2}^{\beta \beta}\right)_{ii} = \ell_i^{p(\beta,\beta)} p_{\alpha}(\alpha)_i.$$

The expression for Γ_a^{bb} is obtained substituting β and α 's with b and a's, respectively.

• $\Gamma_{\psi_3}^{\alpha\beta}$ (or $(\Gamma_{\psi_3}^{\beta\alpha})^{\mathsf{T}}$) has seven cases. If $\psi_3 \in \{\gamma, \alpha_*, \beta_*, a, b\}$, we have

$$\Gamma_{oldsymbol{\psi}_3}^{oldsymbol{lphaeta}} = \mathbf{M}_{oldsymbol{eta}}^{\mathsf{T}} \mathbf{V}_{oldsymbol{\psi}_3}^{oldsymbol{lphaeta}} \mathbf{M}_{oldsymbol{lpha}} + \left(\mathbf{M}_{oldsymbol{eta}}^1
ight)^{\mathsf{T}} \mathbf{D}_{oldsymbol{\psi}_3} \mathbf{M}_{oldsymbol{lpha}},$$

where

$$(\mathbf{D}_{\boldsymbol{\psi}_3})_{ii} = \ell_i^{p(\boldsymbol{\beta},\boldsymbol{\psi}_3)} p_{\boldsymbol{\psi}_3}(\boldsymbol{\psi}_3)_i.$$

If $\psi_3 \in \{\alpha, \beta\}$ we have

$$\boldsymbol{\Gamma}_{\boldsymbol{\alpha}}^{\boldsymbol{\alpha}\boldsymbol{\beta}} + \boldsymbol{\Gamma}_{\boldsymbol{\beta}}^{\boldsymbol{\alpha}\boldsymbol{\beta}} = \left[\mathbf{M}_{\boldsymbol{\beta}}^{\mathsf{T}} \mathbf{V}_{\boldsymbol{\alpha}\boldsymbol{\beta}1}^{\boldsymbol{\alpha}\boldsymbol{\beta}} + (\mathbf{M}_{\boldsymbol{\beta}}^{1})^{\mathsf{T}} \mathbf{V}_{\boldsymbol{\alpha}\boldsymbol{\beta}2}^{\boldsymbol{\alpha}\boldsymbol{\beta}} + (\mathbf{M}_{\boldsymbol{\beta}}^{2})^{\mathsf{T}} \mathbf{V}_{\boldsymbol{\alpha}\boldsymbol{\beta}3}^{\boldsymbol{\alpha}\boldsymbol{\beta}} \right] \mathbf{M}_{\boldsymbol{\alpha}\boldsymbol{\beta}2}$$

where

$$\left(\mathbf{V}_{\boldsymbol{\alpha}\boldsymbol{\beta}1}^{\boldsymbol{\alpha}\boldsymbol{\beta}}\right)_{ii} = \ell_i^{p(\boldsymbol{\beta},\boldsymbol{\beta},\boldsymbol{\alpha})} p_{\boldsymbol{\beta}}(\boldsymbol{\beta}) + \ell_i^{p(\boldsymbol{\beta},\boldsymbol{\beta})} p_{\boldsymbol{\beta}}^1(\boldsymbol{\beta}) + \ell_i^{p(\boldsymbol{\beta},\boldsymbol{\alpha},\boldsymbol{\alpha})} p_{\boldsymbol{\alpha}}(\boldsymbol{\alpha}),$$

$$\left(\mathbf{V}_{\alpha\beta2}^{\alpha\beta}\right)_{ii} = \ell_i^{p(\beta,\beta)} p_{\beta}(\beta) + 2\ell_i^{p(\beta,\alpha)} p_{\alpha}(\alpha), \qquad (\mathbf{V}_{\alpha\beta3}^{\alpha\beta})_{ii} = \ell_i^{p(\beta)} p_{\alpha}(\alpha).$$

Formulas to compute $\Gamma_{\psi_3}^{\beta\alpha}$ are obtained by transposing $\Gamma_{\psi_3}^{\alpha\beta}$.

• $\Gamma^{ab}_{\psi_3}$ (or $(\Gamma^{ba}_{\psi_3})^{\mathsf{T}}$) has seven cases. When $\psi_3 \in \{\gamma, \alpha, \beta, a_*, b_*\}$ it is analogous to $\Gamma^{\alpha\beta}_{\psi_3}$ (with $\psi_3 \in \{\gamma, \alpha, \beta, a_*, b_*\}$).

The cases $\psi_3 = a$ or **b** are harder, that is,

$$\Gamma_{b}^{ab} = \left[\mathbf{M}_{b}^{\mathsf{T}}\mathbf{V}_{b1}^{ab} + (\mathbf{M}_{b}^{1})^{\mathsf{T}}\mathbf{V}_{b2}^{ab}\right]\mathbf{M}_{a},$$

where

$$\left(\mathbf{V}_{\boldsymbol{b}1}^{\boldsymbol{ab}}\right)_{ii} = \ell_i^{p(\boldsymbol{a},\boldsymbol{b},\boldsymbol{b})} p_{\boldsymbol{b}}(\boldsymbol{b}) + \ell_i^{p(\boldsymbol{b},\boldsymbol{b})} p_{\boldsymbol{b}}^1(\boldsymbol{b}) \qquad \qquad \left(\mathbf{V}_{\boldsymbol{b}2}^{\boldsymbol{ab}}\right)_{ii} = \ell_i^{p(\boldsymbol{b},\boldsymbol{b})} p_{\boldsymbol{b}}(\boldsymbol{b}).$$

While

$$\boldsymbol{\Gamma_a^{ab}} = \left[\boldsymbol{\mathrm{M}_b^\mathsf{T}} \boldsymbol{\mathrm{V}_{a1}^{ab}} + (\boldsymbol{\mathrm{M}_b^1})^\mathsf{T} \boldsymbol{\mathrm{V}_{a2}^{ab}} + (\boldsymbol{\mathrm{M}_b^2})^\mathsf{T} \boldsymbol{\mathrm{V}_{a3}^{ab}} \right] \boldsymbol{\mathrm{M}_a} + \left[\boldsymbol{\mathrm{M}_b^\mathsf{T}} + (\boldsymbol{\mathrm{M}_b^1})^\mathsf{T} \right] \boldsymbol{\mathrm{V}_{a4}^{ab}} \boldsymbol{\mathrm{P}_a^1},$$

where

Formulas to compute $\Gamma_{\psi_3}^{ba}$ are obtained by transposing $\Gamma_{\psi_3}^{ab}$.

• $\Gamma^{aa}_{\psi_3}$ has seven cases. When $\psi_3 = a$ it must be computed via

$$\Gamma_{a}^{aa} = \mathbf{M}_{\mathbf{a}}^\mathsf{T} \mathbf{V}_{a1}^{aa} \mathbf{M}_{\mathbf{a}} + \mathbf{M}_{\mathbf{a}}^\mathsf{T} \mathbf{V}_{a2}^{aa} \mathbf{P}_{a}^1 + \left(\mathbf{M}_{\mathbf{a}}^\mathsf{T} \mathbf{V}_{a2}^{aa} \mathbf{P}_{a}^1\right)^\mathsf{T} + \mathbf{V}_{a3}^{aa} + \mathbf{V}_{a4}^{aa}$$

where

$$\begin{split} \left(\mathbf{V}_{\boldsymbol{a}1}^{\boldsymbol{a}\boldsymbol{a}}\right)_{ii} &= \ell_{i}^{p(\boldsymbol{a},\boldsymbol{a},\boldsymbol{a})} p_{\boldsymbol{a}}(\boldsymbol{a})_{i}, \\ \left(\mathbf{V}_{\boldsymbol{a}2}^{\boldsymbol{a}\boldsymbol{a}}\right)_{jk} &= \sum_{i=1}^{n} \left(\ell_{i}^{p(\boldsymbol{a},\boldsymbol{a})} p_{\boldsymbol{a}}(\boldsymbol{a})_{i}\right) \left(\mathbf{M}_{\boldsymbol{a}}^{1}\right)_{ijk}, \\ \left(\mathbf{V}_{\boldsymbol{a}3}^{\boldsymbol{a}\boldsymbol{a}}\right)_{jk} &= \sum_{i=1}^{n} \ell_{i}^{p(\boldsymbol{a})} \left(\mathbf{P}_{\boldsymbol{a}}^{2}\right)_{ijk}. \end{split}$$

Note that the last term requires $O(np_a^3)$ computation. The case where $\psi_3 = \boldsymbol{b}$ is

$$\Gamma_b^{aa} = \mathbf{M_a^\mathsf{T}} \mathbf{V_{b1}^{aa}} \mathbf{M_a} + \mathbf{V_{b2}^{aa}}$$

where

$$(\mathbf{V}_{\boldsymbol{b}1}^{\boldsymbol{a}\boldsymbol{a}})_{ii} = \ell_i^{p(\boldsymbol{a},\boldsymbol{a},\boldsymbol{b})} p_{\boldsymbol{b}}(\boldsymbol{b})_i + 2\ell_i^{p(\boldsymbol{a},\boldsymbol{b})} p_{\boldsymbol{b}}^1(\boldsymbol{b})_i + \ell_i^{p(\boldsymbol{b})} p_{\boldsymbol{b}}^2(\boldsymbol{b})_i; ,$$

$$(\mathbf{V}_{\boldsymbol{b}2}^{\boldsymbol{a}\boldsymbol{a}})_{jk} = \left(\ell_i^{p(\boldsymbol{a},\boldsymbol{b})} p_{\boldsymbol{b}}(\boldsymbol{b})_i + \ell_i^{p(\boldsymbol{b})} p_{\boldsymbol{b}}^1(\boldsymbol{b})_i\right) \left(\mathbf{M}_{\boldsymbol{a}}^1\right)_{ijk}.$$

To compute \mathbf{V}_{b2}^{aa} we first compute $\sum_{i=1}^{n} \left(\ell_i^{p(a,b)} p_b(b)_i + \ell_i^{p(b)} p_b^1(b)_i \right)$ which is $O(np_b)$ and then multiply by $(\mathbf{M}_a^1)_{ijk}$ which is $O(np_a^2)$. The case where $\psi_3 \neq a, b$ is

$$\Gamma_{\psi_3}^{aa} = \mathbf{M}_{\mathbf{a}}^\mathsf{T} \mathbf{V}_{\psi_31}^{aa} \mathbf{M}_{\mathbf{a}} + \mathbf{V}_{\psi_32}^{aa}$$

where

$$\left(\mathbf{V}_{\boldsymbol{\psi}_{3}1}^{\boldsymbol{a}\boldsymbol{a}}\right)_{ii} = \ell_{i}^{p(\boldsymbol{a},\boldsymbol{a},\boldsymbol{\psi}_{3})}, \qquad \left(\mathbf{V}_{\boldsymbol{\psi}_{3}2}^{\boldsymbol{a}\boldsymbol{a}}\right)_{jk} = \sum_{i=1}^{n} \left(\ell_{i}^{p(\boldsymbol{a},\boldsymbol{\psi}_{3})} p_{\boldsymbol{\psi}_{3}}(\boldsymbol{\psi}_{3})_{i}\right) \left(\mathbf{M}_{\boldsymbol{a}}^{1}\right)_{ijk}.$$

• $\Gamma_a^{a\psi_2}$ with $\psi_2 \neq a, b$ is

$$\Gamma_{m{a}}^{m{a}m{\psi}_2} = \mathbf{M}_{m{\psi}_2}^\mathsf{T} \mathbf{V}_{m{a}1}^{m{a}m{\psi}_2} \mathbf{M}_{m{\psi}_1} + \mathbf{M}_{m{\psi}_2}^\mathsf{T} \mathbf{V}_{m{a}2}^{m{a}m{\psi}_2} \mathbf{P}_{m{a}2}^1$$

where

$$\left(\mathbf{V}_{a1}^{a\psi_2}\right)_{ii} = \ell_i^{p(a,a,\psi_2)} p_a(a)_i, \qquad \left(\mathbf{V}_{a2}^{a\psi_2}\right)_{ii} = \ell_i^{p(a,\psi_2)}.$$

• For the triplets $\Gamma_{\beta}^{\psi_1 \alpha}$ (or $(\Gamma_{\beta}^{\alpha \psi_1})^{\mathsf{T}}$) with $\psi_1 \neq \alpha, \beta$ and $\Gamma_{b}^{\psi_1 a}$ (or $(\Gamma_{b}^{a \psi_1})^{\mathsf{T}}$) with $\psi_1 \neq a, b$ we have

$$\Gamma_{\boldsymbol{\beta}}^{\psi_1 \boldsymbol{\alpha}} = \mathbf{M}_{\boldsymbol{\alpha}}^\mathsf{T} \left(\mathbf{V}_{\boldsymbol{\beta}}^{\psi_1 \boldsymbol{\alpha}} + \mathbf{E}_{\boldsymbol{\beta}}^{\psi_1} \right) \mathbf{M}_{\psi_1},$$

with

$$\left(\mathbf{E}_{\boldsymbol{\beta}}^{\boldsymbol{\psi}_1}\right)_{ii} = \ell_i^{p(\boldsymbol{\psi}_1,\boldsymbol{\beta})} p_{\boldsymbol{\beta}}^1(\boldsymbol{\beta})_i.$$

The formula for $\Gamma_b^{\psi_1 a}$ is obtained by substituting a and b to α and β , respectively. The formulas for $\Gamma_{\beta}^{\alpha\psi_1}$ and $\Gamma_b^{a\psi_1}$ are computed by transposing $\Gamma_{\beta}^{\psi_1 \alpha}$ and $\Gamma_b^{\psi_1 a}$. The triplets of the form $\Gamma_{\alpha}^{\psi_1 \beta}$ (or $(\Gamma_{\alpha}^{\beta\psi_1})^{\mathsf{T}}$) (with $\psi_1 \neq \alpha, \beta$) and $\Gamma_a^{\psi_1 b}$ (or $(\Gamma_a^{b\psi_1})^{\mathsf{T}}$) (with $\psi_1 \neq a, b$), can be computed as follows

$$\Gamma_{m{lpha}}^{\psi_1m{eta}} = \mathbf{M}_{m{eta}}^{\mathsf{T}} \mathbf{V}_{m{lpha}}^{\psi_1m{eta}} \mathbf{M}_{\psi_1} + \mathbf{G}_{m{lpha}}^{\psi_1m{eta}},$$

where

$$\mathbf{G}_{\boldsymbol{\alpha}}^{\psi_1 \boldsymbol{\beta}} = \left(\mathbf{M}_{\boldsymbol{\beta}}^1\right)^\mathsf{T} \mathbf{F}_{\boldsymbol{\alpha}}^{\psi_1 \boldsymbol{\beta}} \mathbf{M}_{\psi_1}, \qquad \left(\mathbf{F}_{\boldsymbol{\alpha}}^{\psi_1 \boldsymbol{\beta}}\right)_{ii} = \ell_i^{p(\psi_1, \boldsymbol{\beta})} p_{\boldsymbol{\alpha}}(\boldsymbol{\alpha})_i.$$

S3 Log-likelihood derivatives with respect to η and \tilde{s}

To compute the derivative of the log-likelihood with respect to the coefficients and smoothing parameters, we apply the chain rule. This requires the partial derivatives of the log-likelihood ℓ with respect to the linear predictors η and the nested effects \tilde{s} . The first-order partial derivative of ℓ with respect to a general linear predictor η is given by:

$$\ell^{\eta} = \frac{\partial \ell}{\partial \eta} = \ell^{\theta} \theta^{\eta},$$

where $\theta^{\eta} = \partial \theta / \partial \eta$ is the first derivative of the inverse link function. The higher-order derivatives are:

$$\ell^{\eta\eta} = \ell^{\theta}\theta^{\eta\eta} + \ell^{\theta\theta}(\theta^{\eta})^{2}, \qquad \qquad \ell^{\eta\eta\eta} = \ell^{\theta}\theta^{\eta\eta\eta} + 3\ell^{\theta\theta}\theta^{\eta}\theta^{\eta\eta} + \ell^{\theta\theta\theta}(\theta^{\eta})^{3}.$$

For a nested effect \tilde{s} the first-order partial derivative is given by:

$$\ell^{\tilde{s}} = \frac{\partial \ell}{\partial \tilde{s}} = \ell^{\eta} \eta^{\tilde{s}},$$

where $\eta^{\tilde{s}} = (\mathbf{m_b^1})^T \boldsymbol{\gamma}$ with $\mathbf{m_b^1}$ representing a row of $\mathbf{M_b^1}$ (substitute **b** with $\boldsymbol{\beta}$ for a single index effect). The pattern for $\ell^{\tilde{s}\tilde{s}}$ and $\ell^{\tilde{s}\tilde{s}\tilde{s}}$ follows the same structure as $\ell^{\eta\eta}$ and $\ell^{\eta\eta\eta}$, with substitutions $\ell^{\eta} \to \ell^{\tilde{s}}$, $\ell^{\theta} \to \ell^{\eta}$, $\theta^{\eta} \to \eta^{\tilde{s}}$, $\theta^{\eta\eta} \to \eta^{\tilde{s}\tilde{s}}$, and $\theta^{\eta\eta\eta} \to \eta^{\tilde{s}\tilde{s}\tilde{s}}$. The mixed derivatives are then given by:

$$\ell^{\eta \tilde{s}} = \ell^{\eta \eta} \eta^{\tilde{s}}, \qquad \qquad \ell^{\eta \eta \tilde{s}} = \ell^{\eta \eta \eta} \eta^{\tilde{s}}, \qquad \qquad \ell^{\eta \tilde{s} \tilde{s}} = \ell^{\eta \eta \eta} (\eta^{\tilde{s}})^2 + \ell^{\eta \eta} \eta^{\tilde{s} \tilde{s}}.$$

S4 Derivatives of \tilde{s} with respect to a

If \tilde{s} is a linear combination, then all derivatives of order higher than 1 are zero, and the gradient is simply the matrix of inner covariates, i.e., $\frac{\partial \tilde{s}(\mathbf{x})}{\partial a} = \mathbf{x}$. For the remainder of this section, we will focus on the case where \tilde{s} is an adaptive exponential smoothing or a multivariate kernel smoothing. In Section S1, the centred and scaled nested effect is defined as:

$$\tilde{s}'(\mathbf{x}) = e^{a_0}(\tilde{s}(\mathbf{x}) - \bar{\tilde{s}}(\mathbf{x})).$$
 (S4)

By differentiating this equation, we obtain:

$$\frac{\partial \tilde{s}(\mathbf{x})}{\partial a_{j}} = \begin{cases} \tilde{s}(\mathbf{x}) & j = 0 \\ e^{a_{0}} \left(\frac{\partial \tilde{s}(\mathbf{x})}{\partial a_{j}} - n^{-1} \sum_{i=1}^{n} \frac{\partial \tilde{s}(\mathbf{x}_{i})}{\partial a_{j}} \right) & \text{otherwise} \end{cases}$$

$$\frac{\partial^{2} \tilde{s}(\mathbf{x})}{\partial a_{j} \partial a_{k}} = \begin{cases} \frac{\partial \tilde{s}(\mathbf{x})}{\partial a_{j}} & k = 0 \\ e^{a_{0}} \left(\frac{\partial^{2} \tilde{s}(\mathbf{x})}{\partial a_{j} \partial a_{k}} - n^{-1} \sum_{i=1}^{n} \frac{\partial^{2} \tilde{s}(\mathbf{x}_{i})}{\partial a_{j} \partial a_{k}} \right) & \text{otherwise} \end{cases}$$

$$\frac{\partial^{3} \tilde{s}(\mathbf{x})}{\partial a_{j} \partial a_{k} \partial a_{l}} = \begin{cases} \frac{\partial^{2} \tilde{s}(\mathbf{x})}{\partial a_{j} \partial a_{k}} & l = 0 \\ e^{a_{0}} \left(\frac{\partial^{3} \tilde{s}(\mathbf{x})}{\partial a_{i} \partial a_{k} \partial a_{l}} - n^{-1} \sum_{i=1}^{n} \frac{\partial^{3} \tilde{s}(\mathbf{x}_{i})}{\partial a_{j} \partial a_{k} \partial a_{l}} \right) & \text{otherwise} \end{cases}$$

With abuse of notation, the first row of each derivative expression holds up to a permutation of the differentiation order. It is important to note that all the expressions above are written in terms of the derivatives of \tilde{s} . In the following paragraphs, we provide the formulas for computing $\partial \tilde{s}/\partial a_i$, $\partial^2 \tilde{s}/\partial a_i \partial a_k$, and $\partial^3 \tilde{s}/\partial a_i \partial a_k \partial a_l$, specific to each nested effect definition.

S4.1 Adaptive exponential smoothing

Recall the adaptive exponential smoothing definition given in Section 2.2.1:

$$\tilde{s}(z_i) = \tilde{s}_i = \begin{cases} \omega_i \tilde{s}_{i-1} + (1 - \omega_i) z_i & i > 1\\ \omega_i z_0 + (1 - \omega_i) z_1 & i = 1 \end{cases}$$

where z_0 is fixed to some value and $\omega_i \in (0,1)$. The $\omega_i's$ are modelled by $\omega_i = \phi(\tilde{\mathbf{x}}_i^{\mathsf{T}} \boldsymbol{a})$ where $\phi(\cdot)$ is the logistic function. To simplify the notation, denote the derivative with respect to the j-th parameter in vector \boldsymbol{a} using a superscript, e.g., $\tilde{\boldsymbol{s}}^j = \frac{\partial \tilde{\boldsymbol{s}}}{\partial a_j}$. Assuming that z_0 is fixed and known, the derivatives of \tilde{s}_i w.r.t. a_j are

$$\tilde{s}_{i}^{j} = \begin{cases} \omega_{i}^{j}(\tilde{s}_{i-1} - z_{i}) + \omega_{i}\tilde{s}_{i-1}^{j} & i > 1\\ \omega_{1}^{j}(z_{0} - z_{1}) & i = 1 \end{cases}$$

$$\tilde{s}_{i}^{jk} = \begin{cases} \omega_{i}^{jk}(\tilde{s}_{i-1} - z_{i}) + \omega_{i}^{j}\tilde{s}_{i-1}^{k} + \omega_{i}^{k}\tilde{s}_{i-1}^{j} + \omega_{i}\tilde{s}_{i-1}^{jk} & i > 1\\ \omega_{1}^{jk}(z_{0} - z_{1}) & i = 1 \end{cases}$$

$$\tilde{s}_{i}^{jkl} = \begin{cases} \omega_{i}^{jkl}(\tilde{s}_{i-1} - z_{i}) + \omega_{i}^{jk}\tilde{s}_{i-1}^{l} + \omega_{i}^{jl}\tilde{s}_{i-1}^{k} + \omega_{i}^{kl}\tilde{s}_{i-1}^{j} +\\ + \omega_{i}^{j}\tilde{s}_{i-1}^{kl} + \omega_{i}^{k}\tilde{s}_{i-1}^{jl} + \omega_{i}\tilde{s}_{i-1}^{jk} + \omega_{i}\tilde{s}_{i-1}^{jkl} + \omega_{i}\tilde{s}_{i-1}^{jkl} \\ \omega_{1}^{jkl}(z_{0} - z_{1}) & i = 1 \end{cases}$$

where

$$\omega_i^j = \phi_i' \tilde{X}_{ij}, \qquad \qquad \omega_i^{jk} = \phi_i'' \tilde{X}_{ij} \tilde{X}_{ik}, \qquad \qquad \omega_i^{jk} = \phi_i''' \tilde{X}_{ij} \tilde{X}_{ik} \tilde{X}_{il}.$$

S4.2 Multivariate kernel smoothing

Denoting by K_a the Kernel of a multivariate density function parameterized by the vector \mathbf{a} , and by z_{ij} the scalar covariate corresponding to the vector \mathbf{x}_{ij} , the multivariate kernel smoothing nested effect defined in (4) can be interpreted as a linear transformation:

$$\tilde{s}_i = \boldsymbol{\kappa}_i^{\mathsf{T}} \mathbf{z}_i = \frac{\sum_{u=1}^{n_u} K_{\boldsymbol{a}}(\mathbf{x}_i, \mathbf{x}_{iu}) z_{iu}}{\sum_{q=1}^{n_j} K_{\boldsymbol{a}}(\mathbf{x}_i, \mathbf{x}_{iq})} \quad \text{with} \quad \kappa_{iu} = \frac{K_{\boldsymbol{a}}(\mathbf{x}_i, \mathbf{x}_{iu})}{\sum_{q=1}^{n_j} K_{\boldsymbol{a}}(\mathbf{x}_i, \mathbf{x}_{iq})}$$

The point at which we evaluate the smooth is \mathbf{x}_i . We simplify notation by eliminating index i and the dependency of K on \boldsymbol{a} , so $K_u = K_{\boldsymbol{a}}(\mathbf{x}_i, \mathbf{x}_{iu})$. The u-th element of the first derivative of κ with respect to \boldsymbol{a} is

$$\kappa_{u}^{j} = \frac{\partial \kappa_{u}}{\partial a_{j}} = \frac{K_{u}^{j} \sum_{f=1}^{n_{j}} K_{f} - K_{u} \sum_{f=1}^{n_{j}} K_{f}^{j}}{(\sum_{q=1}^{n_{j}} K_{q})^{2}} = \frac{K_{u}^{j}}{\sum_{q=1}^{n_{j}} K_{q}} - \kappa_{u} \frac{\sum_{f=1}^{n_{j}} K_{f}^{j}}{\sum_{q=1}^{n_{j}} K_{q}}$$

$$= \frac{K_{u}^{j}}{K_{u}} \kappa_{u} - \kappa_{u} \sum_{f=1}^{n_{j}} \left(\frac{K_{f}^{j}}{\sum_{q=1}^{n_{j}} K_{q}} \frac{K_{f}}{K_{f}} \right) = L_{u}^{j} \kappa_{u} - \kappa_{u} \sum_{f=1}^{n_{j}} \left(\frac{\kappa_{f} K_{f}^{j}}{K_{f}} \right)$$

$$= \kappa_{u} \left(L_{u}^{j} - \sum_{f=1}^{n_{j}} \kappa_{f} L_{f}^{j} \right),$$

where $L_u = \log K_u$ implying that $L_u^j = \frac{K_u^j}{K_u}$. The second derivative is

$$\kappa_u^{jk} = \kappa_u^k \left(L_u^j - \sum_{f=1}^{n_j} \kappa_f L_f^j \right) + \kappa_u \left(L_u^{jk} - \sum_{f=1}^{n_j} \kappa_f^k L_f^j - \sum_{f=1}^{n_j} \kappa_f L_f^{jk} \right).$$

Assuming that K_a is an unnormalized Gaussian kernel, for $k \neq j$, κ_u^{jk} simplifies to

$$\kappa_u^{jk} = \kappa_u^k \left(L_u^j - \sum_{f=1}^{n_j} \kappa_f L_f^j \right) - \kappa_u \sum_{f=1}^{n_j} \kappa_f^k L_f^j, \qquad (Gaussian case, k \neq j).$$

Finally, the third-order derivative is

$$\kappa_{u}^{jkl} = \kappa_{u}^{kl} \left(L_{u}^{j} - \sum_{f=1}^{n_{j}} \kappa_{f} L_{f}^{j} \right) + \kappa_{u}^{k} \left(L_{u}^{jl} - \sum_{f=1}^{n_{j}} \kappa_{f}^{l} L_{f}^{j} - \sum_{f=1}^{n_{j}} \kappa_{f} L_{f}^{jl} \right) +$$

$$+ \kappa_{u}^{l} \left(L_{u}^{jk} - \sum_{f=1}^{n_{j}} \kappa_{f}^{k} L_{f}^{j} - \sum_{f=1}^{n_{j}} \kappa_{f} L_{f}^{jk} \right) +$$

$$+ \kappa_{u} \left(L_{u}^{jkl} - \sum_{f=1}^{n_{j}} \kappa_{f}^{kl} L_{f}^{j} - \sum_{f=1}^{n_{j}} \kappa_{f}^{k} L_{f}^{jl} - \sum_{f=1}^{n_{j}} \kappa_{f}^{l} L_{f}^{jk} - \sum_{f=1}^{n_{j}} \kappa_{f} L_{f}^{jkl} \right),$$

which, if K_a is an unnormalized Gaussian kernel and $j \neq k \land j \neq l \land k \neq l$ simplifies to

$$\kappa_u^{jkl} = \kappa_u^{kl} \left(L_u^j - \sum_{f=1}^{n_j} \kappa_f L_f^j \right) - \kappa_u^k \sum_{f=1}^{n_j} \kappa_f^l L_f^j - \kappa_u^l \sum_{f=1}^{n_j} \kappa_f^k L_f^j - \kappa_u \sum_{f=1}^{n_j} \kappa_f^{kl} L_f^j.$$
 (S5)

If $j = k \neq l$ or $j = l \neq k$, we need to add the following terms to (S5):

$$\kappa_u^l \left(L_u^{jj} - \sum_{f=1}^{n_j} \kappa f L_f^{jj} \right) - \kappa_u \sum_{f=1}^{n_j} \kappa f^l L_f^{jj}, \quad \text{or} \quad \kappa_u^k \left(L_u^{jj} - \sum_{f=1}^{n_j} \kappa f L_f^{jj} \right) - \kappa_u \sum_{f=1}^{n_j} \kappa f^k L_f^{jj}.$$

If j = k = l, we add both of the above terms as well as the following:

$$\kappa_u \left(L_u^{jjj} - \sum_{f=1}^{n_j} \kappa_f L_f^{jjj} \right).$$

S4.2.1 Derivatives of independent multivariate Gaussian kernel

Consider the special case where observations are assumed to be independent. Define $m(\mathbf{x} \mid \boldsymbol{\mu}, \boldsymbol{\sigma})$ as the log-kernel of a multivariate normal with mean $\boldsymbol{\mu}$ and covariance diag($\boldsymbol{\sigma}^2$). Let $\boldsymbol{\rho} = -\log \boldsymbol{\sigma}$. Thus

$$m = m(x_i \mid \mu_i, \rho_i) = -(x_i - \mu_i)^2 e^{2\rho_i},$$

and

$$m^{j} = \frac{\partial m}{\partial \rho_{j}} = 2m,$$
 $m^{jj} = 2m^{j},$ $m^{jjj} = 2m^{jj}$

and so forth, where mixed derivative with respect to ρ_j and ρ_k equal zero.

S5 Derivatives of scaling penalty with respect to a

In Section S1 introduced a penalty $q(\zeta)$ on the observed variance of the nested effect \tilde{s} . This approach addresses the scaling problem described in Section 2.3 by ensuring that the empirical variance $v\hat{a}r(\tilde{s})$ of \tilde{s} remains constant at c. Below, we provide the derivatives for both a general nested effect and a single index effect, the latter being computationally more efficient due to its linear structure.

S5.1 General case

Recall the penalty definition given in Section S1:

$$q_{\tilde{s}'} = (\hat{var}[\tilde{s}'(\mathbf{x})] - c)^2.$$

where $\hat{\mathbf{var}}(\tilde{\mathbf{s}}')$ represents the sample variance of $\tilde{\mathbf{s}}'$, and c > 0 is a constant. To keep the notation simple, in this section $\tilde{\mathbf{s}}$ denotes the scaled inner transformation, i.e. $e^{a_0}\tilde{\mathbf{s}}$. As in the previous sections, let f^j represent the partial derivative of a function f with respect to the j-th parameter. Higher-order derivatives are indicated with additional superscript letters. Consequently, $q_{\tilde{\mathbf{s}}'}^j$ is given by

$$q_{\tilde{s}'}^{j} = \frac{\partial q_{\tilde{s}'}}{\partial a_{j}} = \frac{4}{n} \left(\hat{\text{var}}(\tilde{s}') - c \right) \sum_{i=1}^{n} \left(\tilde{s}_{i} - \overline{\tilde{s}} \right) \left(\tilde{s}_{i}^{j} - \overline{\tilde{s}^{j}} \right)$$
$$= \frac{4}{n} \left(\hat{\text{var}}(\tilde{s}') - c \right) \sum_{i=1}^{n} \tilde{s}_{ci} \tilde{s}_{ci}^{j}$$

or in vector form:

$$\nabla_{\boldsymbol{a}} q_{\tilde{\boldsymbol{s}}'} = \frac{4}{n} \{ \hat{\mathbf{var}}(\tilde{\boldsymbol{s}}') - c \} \bar{\mathbf{U}}^{\mathsf{T}} \tilde{\boldsymbol{s}}_c$$

where $\bar{\mathbf{U}} = \nabla_{\boldsymbol{a}}\tilde{\boldsymbol{s}} - \mathbf{1}\mathbf{1}^{\mathsf{T}}\nabla_{\boldsymbol{a}}\tilde{\boldsymbol{s}}$, with $\mathbf{1} = \{1, \dots, 1\}$, denote the column-centred version of the Jacobian $\nabla_{\boldsymbol{a}}\tilde{\boldsymbol{s}}$, and $\tilde{\boldsymbol{s}}_{ci} = \tilde{\boldsymbol{s}}_i - \bar{\tilde{\boldsymbol{s}}} = \tilde{\boldsymbol{s}}_i - \mathbf{1}^{\mathsf{T}}\tilde{\boldsymbol{s}}$ represents the *i*-th element of centered nested effect (similar notation is adopted for higher-order derivatives). The jk element of the Hessian matrix is

$$q_{\tilde{s}'}^{jk} = \frac{8}{n^2} \sum_{i=1}^n \tilde{s}_{ci} \tilde{s}_{ci}^j \sum_{i=1}^n \tilde{s}_{ci} \tilde{s}_{ci}^k + \frac{4}{n} \left(\hat{\text{var}}(\tilde{s}') - c \right) \left(\sum_{i=1}^n \tilde{s}_{ci}^k \tilde{s}_{ci}^j + \sum_{i=1}^n \tilde{s}_{ci} \tilde{s}_{ci}^{jk} \right).$$

In matrix form

$$\nabla_{\boldsymbol{a}}^{\mathsf{T}} \nabla_{\boldsymbol{a}} q_{\tilde{\boldsymbol{s}}'} = \frac{4}{n} \left[\frac{2}{n} \bar{\mathbf{U}}^{\mathsf{T}} \tilde{\boldsymbol{s}}_c \tilde{\boldsymbol{s}}_c^{\mathsf{T}} \bar{\mathbf{U}} + (\hat{\operatorname{var}}(\tilde{\boldsymbol{s}}') - c)(\bar{\mathbf{U}}^{\mathsf{T}} \bar{\mathbf{U}} + \mathbf{P}) \right],$$

where $\mathbf{P} = \sum_{i=1}^{n} \tilde{s}_{ci} \nabla_{\mathbf{a}}^{\mathsf{T}} \nabla_{\mathbf{a}} \tilde{s}_{ci}$. The third derivative is

$$q_{\tilde{s}'}^{jkl} = \frac{8}{n^2} \left(\sum_{i=1}^n \left(\tilde{s}_{ci}^l \tilde{s}_{ci}^j + \tilde{s}_{ci} \tilde{s}_{ci}^{jl} \right) \sum_{i=1}^n \tilde{s}_{ci} \tilde{s}_{ci}^k + \sum_{i=1}^n \tilde{s}_{ci} \tilde{s}_{ci}^j \sum_{i=1}^n \left(\tilde{s}_{ci}^l \tilde{s}_{ci}^k + \tilde{s}_{ci} \tilde{s}_{ci}^{kl} \right) \right) +$$

$$+ \frac{4}{n} \left[\frac{2}{n} \sum_{i=1}^n \tilde{s}_{ci} \tilde{s}_{ci}^l \left(\sum_{i=1}^n \tilde{s}_{ci}^k \tilde{s}_{ci}^j + \sum_{i=1}^n \tilde{s}_{ci} \tilde{s}_{ci}^{jk} \right) +$$

$$+ (\hat{var}(\tilde{s}') - c) \left(\sum_{i=1}^n \tilde{s}_{ci}^{kl} \tilde{s}_{ci}^j + \sum_{i=1}^n \tilde{s}_{ci}^k \tilde{s}_{ci}^{jl} + \sum_{i=1}^n \tilde{s}_{ci}^l \tilde{s}_{ci}^{jk} + \sum_{i=1}^n \tilde{s}_{ci} \tilde{s}_{ci}^{jk} \right) \right].$$

Defining $\mathbf{q} = \bar{\mathbf{U}}^{\mathsf{T}} \tilde{\mathbf{s}}_c$, $\mathbf{C} = \bar{\mathbf{U}}^{\mathsf{T}} \bar{\mathbf{U}}$ and the 3D arrays \mathbf{A} and \mathbf{B} such that $A_{abc} = q_a (C_{bc} + P_{bc})$ and $B_{abc} = \sum_{i=1}^n \tilde{\mathbf{s}}_{ci}^a \tilde{\mathbf{s}}_{ci}^{bc}$, the aforementioned expression can be reformulated as

$$q_{\tilde{s}'}^{jkl} = \frac{8}{n^2} \left(A_{jkl} + A_{kjl} + A_{ljk} \right) + \frac{4}{n} (\hat{var}(\tilde{s}') - c) \left(B_{jkl} + B_{kjl} + B_{ljk} + \sum_{i=1}^{n} \tilde{s}_{ci} \tilde{s}_{ci}^{jkl} \right).$$

Note that A_{abc} and B_{abc} are symmetric in b and c but not in a (i.e., $A_{abc} = A_{acb}$ but $A_{abc} \neq A_{cba}$). Additionally, the derivative of $\nabla_{\boldsymbol{a}}^{\mathsf{T}} \nabla_{\boldsymbol{a}} q_{\tilde{s}'}$ with respect to log-smoothing parameter ρ is required. This is

$$\frac{\mathrm{d}q_{\tilde{s}'}^{jk}}{\mathrm{d}\rho} = q_{\tilde{s}'}^{jkl} \frac{\mathrm{d}\hat{a}_{l}}{\mathrm{d}\rho}
= \frac{8}{n^{2}} \left((\mathbf{C} + \mathbf{P}) \boldsymbol{a}_{\rho} \mathbf{q}^{\mathsf{T}} + \mathbf{q} \mathbf{a}_{\rho}^{\mathsf{T}} (\mathbf{C} + \mathbf{P}) + \mathbf{q}^{\mathsf{T}} \boldsymbol{a}_{\rho} (\mathbf{C} + \mathbf{P}) \right) +
+ \frac{4}{n} (\hat{var}(\tilde{s}') - c) \left(\mathbf{Z}^{\mathsf{T}} \mathbf{U} + \mathbf{Z} \mathbf{U}^{\mathsf{T}} + \sum_{i=1}^{n} (\mathbf{U} \boldsymbol{a}_{\rho})_{i} \tilde{s}_{ci}^{jk} + \sum_{i=1}^{n} \tilde{s}_{ci} \sum_{l=1}^{n} \tilde{s}_{ci}^{jkl} (\boldsymbol{a}_{\rho})_{l} \right),$$

where $(\boldsymbol{a}_{\rho})_{l} = \frac{\mathrm{d}\hat{a}_{l}}{\mathrm{d}\rho}$ and **Z** is such that $Z_{ia} = \sum_{l=1}^{n} \tilde{s}_{ci}^{al} \frac{\mathrm{d}\hat{a}_{l}}{\mathrm{d}\rho}$.

S5.2 Single index case

For the single index case, the linearity of the effect results in some terms being zero, allowing more efficient computations. The derivatives of $q_{\tilde{s}'}$ are

$$q_{\tilde{s}'}^{j} = 4 \left(\hat{\text{var}}(\tilde{\mathbf{X}}\boldsymbol{a}) - c \right) \hat{\boldsymbol{\sigma}}_{j}^{\mathsf{T}} \boldsymbol{a},$$

$$q_{\tilde{s}'}^{jk} = 8 \hat{\boldsymbol{\sigma}}_{j}^{\mathsf{T}} \boldsymbol{a} \boldsymbol{a}^{\mathsf{T}} \hat{\boldsymbol{\sigma}}_{k} + 4 \left(\hat{\text{var}}(\tilde{\mathbf{X}}\boldsymbol{a}) - c \right) \hat{\boldsymbol{\sigma}}_{jk},$$

$$q_{\tilde{s}'}^{jkl} = 8 \left(\hat{\sigma}_{jl} \boldsymbol{a}^{\mathsf{T}} \hat{\boldsymbol{\sigma}}_{k} + \hat{\boldsymbol{\sigma}}_{j}^{\mathsf{T}} \boldsymbol{a} \hat{\boldsymbol{\sigma}}_{kl} \right) + 8 \hat{\sigma}_{jk} \hat{\boldsymbol{\sigma}}_{l}^{\mathsf{T}} \boldsymbol{a}$$

$$= 8 \left(\hat{\sigma}_{jl} \{ \hat{\boldsymbol{\Sigma}} \boldsymbol{a} \}_{k} + \hat{\sigma}_{kl} \{ \hat{\boldsymbol{\Sigma}} \boldsymbol{a} \}_{j} + \hat{\sigma}_{jk} \{ \hat{\boldsymbol{\Sigma}} \boldsymbol{a} \}_{l} \right),$$

where $\hat{\boldsymbol{\sigma}}_j$ represents the j-th column or row of $\hat{\boldsymbol{\Sigma}} = \hat{\operatorname{cov}}(\tilde{\mathbf{X}})$, which is the empirical maximum likelihood covariance matrix estimator (i.e., the maximum likelihood version which divides by n, not n-1). The gradient and Hessian in matrix form are

$$\nabla_{\boldsymbol{a}} q_{\tilde{s}'} = 2 \left(\hat{\text{var}}(\tilde{\mathbf{X}}\boldsymbol{a}) - c \right) \nabla_{\boldsymbol{a}} \hat{\text{var}}(\tilde{\mathbf{X}}\boldsymbol{a})$$
$$= 4 \left(\hat{\text{var}}(\tilde{\mathbf{X}}\boldsymbol{a}) - c \right) \hat{\boldsymbol{\Sigma}}\boldsymbol{a},$$
$$\nabla_{\boldsymbol{a}}^{\mathsf{T}} \nabla_{\boldsymbol{a}} q_{\tilde{s}'} = 8 \hat{\boldsymbol{\Sigma}} \boldsymbol{a} \boldsymbol{a}^{\mathsf{T}} \hat{\boldsymbol{\Sigma}} + 4 \left(\hat{\text{var}}(\tilde{\mathbf{X}}\boldsymbol{a}) - c \right) \hat{\boldsymbol{\Sigma}}.$$

Additionally, we also need the derivative of $\nabla_{\boldsymbol{a}}^{\mathsf{T}} \nabla_{\boldsymbol{a}} q_{\tilde{s}'}$ with respect to ρ . This is

$$\frac{\mathrm{d}q_{\tilde{s}'}^{jk}}{\mathrm{d}\rho} = q_{\tilde{s}'}^{jkl} \frac{\mathrm{d}\hat{a}_l}{\mathrm{d}\rho} = \left[8(\hat{\sigma}_{jl} \boldsymbol{a}^\mathsf{T} \hat{\boldsymbol{\sigma}}_k + \hat{\boldsymbol{\sigma}}_j^\mathsf{T} \boldsymbol{a} \hat{\sigma}_{kl}) + 8\hat{\sigma}_{jk} \hat{\boldsymbol{\sigma}}_l^\mathsf{T} \boldsymbol{a} \right] \frac{\mathrm{d}\hat{a}_l}{\mathrm{d}\rho},$$

which can be computed efficiently by doing

$$\frac{\mathrm{d}\nabla_{\boldsymbol{a}}^{\mathsf{T}}\nabla_{\boldsymbol{a}}q_{\tilde{s}'}}{\mathrm{d}\rho} = 8\left[\hat{\boldsymbol{\Sigma}}\boldsymbol{a}\otimes\left(\hat{\boldsymbol{\Sigma}}\frac{\mathrm{d}\hat{\boldsymbol{a}}}{\mathrm{d}\rho}\right)^{\mathsf{T}} + \hat{\boldsymbol{\Sigma}}\frac{\mathrm{d}\hat{\boldsymbol{a}}}{\mathrm{d}\rho}\otimes(\hat{\boldsymbol{\Sigma}}\boldsymbol{a})^{\mathsf{T}} + \hat{\boldsymbol{\Sigma}}\boldsymbol{a}^{\mathsf{T}}\hat{\boldsymbol{\Sigma}}\frac{\mathrm{d}\hat{\boldsymbol{a}}}{\mathrm{d}\rho}\right].$$

S6 House prices data

In this section, we provide additional details on the covariate definitions and original data sources used to model house prices in London.

- Price Paid Data is a large data set that contains details on all property transactions in England and Wales that were sold for a value and officially recorded by the HM Land Registry. It is available for download from HM Land Registry¹. The data analysed here were obtained by selecting records from the 2022 dataset where city == "LONDON". Furthermore, we concentrated on observations ranging from 100,000 to 10 million pounds. The variables taken into account are:
 - **Postcode**: The postcode at the time of the initial transaction;

¹Contains HM Land Registry data © Crown copyright and database right 2021. This data is licensed under the Open Government Licence v3.0.

- County;
- **Price**: the sale price listed on the transfer deed;
- **Property Type**: D = Detached, S = Semi-Detached, T = Terraced, F = Flats/Maisonettes, O = Other;
- Old/New: Specifies whether the property is newly built (Y) or an older, established building (N);
- **Duration**: refers to the type of tenure: F = Freehold, L = Leasehold;
- PPD Category Type: Indicates the specific category of the price-paid transaction, A = standard price-paid entry, which includes single residential properties sold for value. B = Additional Price Paid entry, such as transfers under a power of sale / possessions, buy-to-let (if identified by a mortgage), transfers to non-private individuals, and sales where the property type is classified as "Other".
- Data on postcode geographical locations can be downloaded from Ordnance Survey National Geographic Database (OS NGD).
- Data on best fit between postcode and Lower Layer Super Output Areas (LSOA) can be downloaded from the Office for National Statistics.
- Index of deprivation 2019 is an index that measures relative deprivation in LSOA. It can be downloaded from the UK government data.
- London Underground station data was sourced from the GitHub repository, available at https://github.com/oobrien.